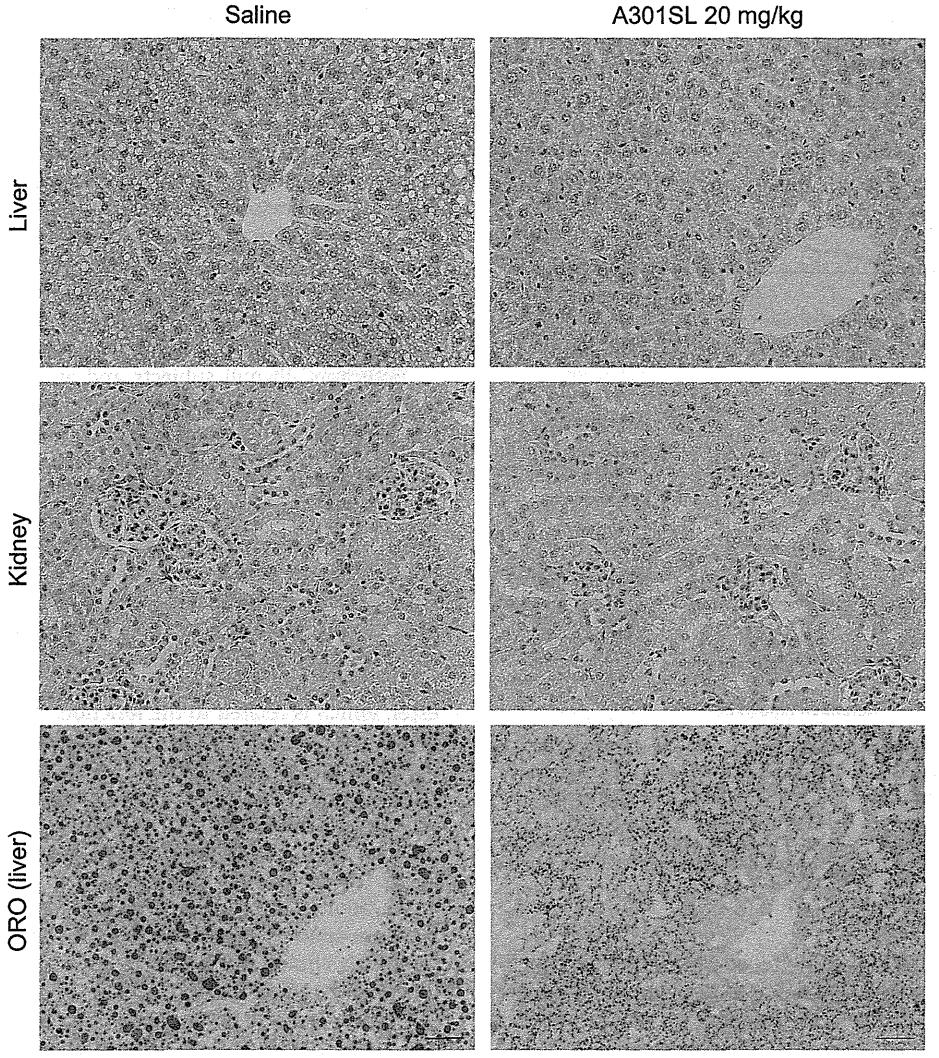

Fig. 5. Representative histopathological changes in livers and kidneys subjected to 16 days of saline (left) and **A301SL** (right) dosing were assessed by H&E or Oil Red O staining (× 200 magnification). Peripheral fatty changes were observed in the liver of the saline-treated mice (top and bottom), while periportal granular degeneration were seen in the highest dose of **A301SL**-treated mice with complete loss of fatty changes (top). No significant changes were observed in kidneys (middle).

Table 3
Histopathological findings.

		Saline	A301SL		A301S
	Dose	–	10 mg/kg	20 mg/kg	20 mg/kg
	Number of mice examined–	9	4	5	5
Organ Liver	Findings				
	Normal	0	3	0	2
	Fatty change, periportal	9	0	0	0
	Granuloma	0	1	1	2
	Granular degeneration, periportal	0	0	5	0
Kidney(s)					
	Normal	9	5	5	4
	Hemorrhage	0	0	0	1

All lesions showed a moderate grade.

Table 4
Effects on serum chemistry.

		AST (IU/L)	ALT (IU/L)	BUN (mg/dL)	Cre (mg/dL)
Saline		17.6 ± 2.8	9.1 ± 3.2	29.7 ± 6.4	0.2 ± 0.05
A301SL	10 mg/kg	22.5 ± 4.6	20 ± 9.2[b]	30.1 ± 4	0.1 ± 0.05
	20 mg/kg	44.2 ± 13.8[b]	14.5 ± 3.3	20.4 ± 3.3[b]	0.1 ± 0.00
A301S	20 mg/kg	22 ± 2	7.5 ± 0.9	18.4 ± 2.6[b]	0.1 ± 0.00

AST; aspartate aminotransferase, ALT; alanine aminotransferase, BUN; blood urea nitrogen, Cre; serum creatinine. Data are presented as means ± S.D.
[a] $P < 0.001$, [c] $P < 0.05$ vs. saline group.
[b] $P < 0.01$ vs. saline group.

showed that our AON does not induce steatosis, which is a typical feature of drug-induced hepatotoxicity (Begriche et al., 2011). Instead, we observed drastic regression of steatohepatitis in **A301SL**-treated arms (Fig. 5), which is presumably an on-target-based pharmacological effect.

In conclusion, we successfully developed an anti-apoC-III LNA–AON. Although this selective apoC-III inhibitor of **A301SL** shows improved potency and safety, it will nevertheless be of help to further elucidate the molecular biology and molecular physiology of apoC-III that other non-selective inhibitors of apoC-III and have failed to reveal.

Acknowledgments and notice of grant support

This work was supported by a Grant-in Aid for Scientific Research from the Japanese Ministry of Health, Labour and Welfare (H23-seisaku tansaku-ippan-004).

References

Applebaum-Bowden, D., Kobayashi, J., Kashyap, V.S., Brown, D.R., Berard, A., Meyn, S., Parrott, C., Maeda, N., Shamburek, R., Brewer, H.B., Santamarina-Fojo, S., 1996. Hepatic lipase gene therapy in hepatic lipase-deficient mice—Adenovirus-mediated replacement of a lipolytic enzyme to the vascular endothelium. J. Clin. Invest. 97, 799–805.

Begriche, K., Massart, J., Robin, M.A., Borgne-Sanchez, A., Fromenty, B., 2011. Drug-induced toxicity on mitochondria and lipid metabolism: mechanistic diversity and deleterious consequences for the liver. J. Hepatol. 54, 773–794.

Bruns, G.A.P., Karathanasis, S.K., Breslow, J.L., 1984. Human apolipoprotein A-I-C-III gene complex is located on chromosome. Arteriosclerosis 4, 97–102.

Busch, S.J., Barnhart, R.L., Martin, G.A., Fitzgerald, M.C., Yates, M.T., Mao, S.J.T., Thomas, C.E., Jackson, R.L., 1994. Human hepatic triglyceride lipase expression reduces high-density-lipoprotein and aortic cholesterol in cholesterol-fed transgenic mice. J. Biol. Chem. 269, 16376–16382.

Clavey, V., Lestaveldelattre, S., Copin, C., Bard, J.M., Fruchart, J.C., 1995. Modulation of lipoprotein B binding to the Ldl receptor by exogenous lipids and apolipoprotein-Ci, apolipoprotein-Cii, apolipoprotein-Ciii, and apolipoprotein-E. Arterioscl. Throm. Vas. 15, 963–971.

Crooke, R.M., Graham, M.J., Lemonidis, K.M., Dobie, K.W., 2009. Modulation of Apolipoprotein C-III Expression. Isis Pharmaceuticals, Inc.. (Isis Pharmaceuticals, I. (Ed.).

Dichek, H.L., Brecht, W., Fan, J.L., Ji, Z.S., McCormick, S.P.A., Akeefe, H., Conzo, L., Sanan, D.A., Weisgraber, K.H., Young, S.G., Taylor, J.M., Mahley, R.W., 1998. Overexpression of hepatic lipase in transgenic mice decreases apolipoprotein B-containing and high density lipoproteins. Evidence that hepatic lipase acts as a ligand for lipoprotein uptake. J. Biol. Chem. 273, 1896–1903.

Fan, J.L., Wang, J.J., Bensadoun, A., Lauer, S.J., Dang, Q., Mahley, R.W., Taylor, J.M., 1994. Overexpression of hepatic lipase in transgenic rabbits leads to a marked reduction of plasma high-density-lipoproteins and intermediate density lipoproteins. Proc. Nat. Acad. Sci. U.S.A. 91, 8724–8728.

Fisher, R.M., Coppack, S.W., Humphreys, S.M., Gibbons, G.F., Frayn, K.N., 1995. Human triacylglycerol-rich lipoprotein subfractions as substrates for lipoprotein lipase. Clin. Chim. Acta 236, 7–17.

Gerritsen, G., Rensen, P.C., Kypreos, K.E., Zannis, V.I., Havekes, L.M., Willems van Dijk, K., 2005. ApoC-III deficiency prevents hyperlipidemia induced by apoE overexpression. J. Lipid Res. 46, 1466–1473.

Goldberg, I.J., 2001. Clinical review 124—diabetic dyslipidemia: causes and consequences. J. Clin. Endocr. Metab. 86, 965–971.

Graham, M.J., Lee, R.G., Bell, T.A., Fu, W.X., Mullick, A.E., Alexander, V.J., Singleton, W., Viney, N., Geary, R., Su, J., Baker, B.F., Burkey, J., Crooke, S.T., Crooke, R.M., 2013. Antisense oligonucleotide inhibition of apolipoprotein C-III reduces plasma triglycerides in rodents, nonhuman primates, and humans. Circ. Res. 112. (1479-U1221).

Grundy, S.M., Brewer, H.B., Cleeman, J.I., Smith, S.C., Lenfant, C., Participants, C., 2004. Definition of metabolic syndrome—Report of the National Heart, Lung, and Blood Institute/American Heart Association Conference on Scientific Issues Related to Definition. Circulation 109, 433–438.

Gupta, N., Fisker, N., Asselin, M.C., Lindholm, M., Rosenbohm, C., Orum, H., Elmen, J., Seidah, N.G., Straarup, E.M., 2010. A locked nucleic acid antisense oligonucleotide (LNA) silences PCSK9 and enhances LDLR expression in vitro and in vivo. PLoS One 5, e10682.

Havel, R.J., Fielding, C.J., Olivecro., T, Shore, V.G., Fielding, P.E., Egelrud, T., 1973. Cofactor activity of protein components of human very low-density lipoproteins in hydrolysis of triglycerides by lipoprotein-lipase from different sources. Biochemistry 12, 1828–1833.

Hokanson, J.E., Austin, M.A., 1996. Plasma triglyceride level is a risk factor for cardiovascular disease independent of high-density lipoprotein cholesterol level: a meta-analysis of population-based prospective studies. J. Cardiovasc. Risk 3, 213–219.

Holmberg, R., Refai, E., Hoog, A., Crooke, R.M., Graham, M., Olivecrona, G., Berggren, P.O., Juntti-Berggren, L., 2011. Lowering apolipoprotein CIII delays onset of type 1 diabetes. Proc. Nat. Acad. Sci. U.S.A. 108, 10685–10689.

Ito, Y., Azrolan, N., O'Connell, A., Walsh, A., Breslow, J.L., 1990. Hypertriglyceridemia as a result of human apo CIII gene expression in transgenic mice. Science 249, 790–793.

Jong, M.C., Rensen, P.C., Dahlmans, V.E., van der Boom, H., van Berkel, T.J., Havekes, L.M., 2001. Apolipoprotein C-III deficiency accelerates triglyceride hydrolysis by lipoprotein lipase in wild-type and apoE knockout mice. J. Lipid Res. 42, 1578–1585.

Juntti-Berggren, L., Larsson, O., Rorsman, P., Ammala, C., Bokvist, K., Wahlander, K., Nicotera, P., Dypbukt, J., Orrenius, S., Hallberg, A., Berggren, P.O., 1993. Increased activity of L-Type Ca^{2+} channels exposed to serum from patients with type-I diabetes. Science 261, 86–90.

Juntti-Berggren, L., Refai, E., Appelskog, I., Andersson, M., Imreh, G., Dekki, N., Uhles, S., Yu, L., Griffiths, W.J., Zaitsev, S., Leibiger, I., Yang, S.N., Olivecrona, G., Jornvall, H., Berggren, P.O., 2004. Apolipoprotein CIII promotes Ca^{2+}-dependent beta cell death in type 1 diabetes. Proc. Nat. Acad. Sci. U.S.A. 101, 10090–10094.

Kinnunen, P.K.J., Ehnholm, C., 1976. Effect of serum and C-apoproteins from very low-density lipoproteins on human postheparin plasma hepatic lipase. FEBS Lett. 65, 354–357.

Lanford, R.E., Hildebrandt-Eriksen, E.S., Petri, A., Persson, R., Lindow, M., Munk, M.E., Kauppinen, S., Orum, H., 2010. Therapeutic silencing of microRNA-122 in primates with chronic hepatitis C virus infection. Science 327, 198–201.

Levin, A.A., 1999. A review of the issues in the pharmacokinetics and toxicology of phosphorothioate antisense oligonucleotides. Biochim. Biophys. Acta 1489, 69–84.

Lindholm, M.W., Elmen, J., Fisker, N., Hansen, H.F., Persson, R., Moller, M.R., Rosenbohm, C., Orum, H., Straarup, E.M., Koch, T., 2012. PCSK9 LNA antisense oligonucleotides induce sustained reduction of LDL cholesterol in nonhuman primates. Mol. Ther. 20, 376–381.

Millar, J.S., Packard, C.J., 1998. Heterogeneity of apolipoprotein B-100-containing lipoproteins: what we have learnt from kinetic studies. Curr. Opin. Lipidol. 9, 197–202.

Milosavljevic, D., Griglio, S., Le Naour, G., Chapman, M.J., 2001. Preferential reduction of very low density lipoprotein-1 particle number by fenofibrate in type IIB hyperlipidemia: consequences for lipid accumulation in human monocyte-derived macrophages. Atherosclerosis 155, 251–260.

Mitsuoka, Y., Kodama, T., Ohnishi, R., Hari, Y., Imanishi, T., Obika, S., 2009. A bridged nucleic acid, 2,4-BNA(COC): synthesis of fully modified oligonucleotides bearing thymine, 5-methylcytosine, adenine and guanine 2,4-BNA(COC) monomers and RNA-selective nucleic-acid recognition. Nucleic Acids Res. 37, 1225–1238.

Miyashita, K., Rahman, S.M.A., Seki, S., Obika, S., Imanishi, T., 2007. N-Methyl substituted 2 ′,4 ′-BNA(NC): a highly nuclease-resistant nucleic acid analogue with high-affinity RNA selective hybridization. Chem. Commun., 3765–3767.

Norata, G.D., Ballantyne, C.M., Catapano, A.L., 2013. New therapeutic principles in dyslipidaemia: focus on LDL and Lp(a) lowering drugs. Eur. Heart J. 34, 1783–1789.

Obika, S., Nanbu, D., Hari, Y., Morio, K., In, Y., Ishida, T., Imanishi, T., 1997. Synthesis of 2′-*O*,4′-C-methyleneuridine and -cytidine. Novel bicyclic nucleosides having a fixed C-3,-endo sugar puckering. Tetrahedron Lett. 38, 8735–8738.

Okazaki, M., Usui, S., Ishigami, M., Sakai, N., Nakamura, T., Matsuzawa, Y., Yamashita, S., 2005. Identification of unique lipoprotein subclasses for visceral obesity by component analysis of cholesterol profile in high-performance liquid chromatography. Arterioscl. Throm. Vas. 25, 578–584.

Ooi, E.M., Barrett, P.H., Chan, D.C., Watts, G.F., 2008. Apolipoprotein C-III: understanding an emerging cardiovascular risk factor. Clin. Sci. (London) 114, 611–624.

Petersen, K.F., Dufour, S., Hariri, A., Nelson-Williams, C., Foo, J.N., Zhang, X.M., Dziura, J., Lifton, R.P., Shulman, G.I., 2010. Apolipoprotein C3 gene variants in nonalcoholic fatty liver disease. N. Engl. J. Med. 362, 1082–1089.

Pollin, T.I., Damcott, C.M., Shen, H., Ott, S.H., Shelton, J., Horenstein, R.B., Post, W., McLenithan, J.C., Bielak, L.F., Peyser, P.A., Mitchell, B.D., Miller, M., O'Connell, J.R., Shuldiner, A.R., 2008. A null mutation in human APOC3 confers a favorable plasma lipid profile and apparent cardioprotection. Science 322, 1702–1705.

Prakash, T.P., Siwkowski, A., Allerson, C.R., Migawa, M.T., Lee, S., Gaus, H.J., Black, C., Seth, P.P., Swayze, E.E., Bhat, B., 2010. Antisense oligonucleotides containing conformationally constrained 2′,4′-(*N*-methoxy)aminomethylene and 2′,4′-*aminooxymethylene and 2′-O,4′-C-aminomethylene bridged nucleoside* analogues show improved potency in animal models. J. Med. Chem. 53, 1636–1650.

Sarwar, N., Danesh, J., Eiriksdottir, G., Sigurdsson, G., Wareham, N., Bingham, S., Boekholdt, S.M., Khaw, K.T., Gudnason, V., 2007. Triglycerides and the risk of coronary heart disease: 10,158 incident cases among 262,525 participants in 29 Western prospective studies. Circulation 115, 450–458.

Sehayek, E., Eisenberg, S., 1991. Mechanisms of inhibition by apolipoprotein C of apolipoprotein-E-dependent cellular-metabolism of human triglyceride-rich lipoproteins through the low-density-lipoprotein receptor pathway. J. Biol. Chem. 266, 18259–18267.

Seth, P.P., Siwkowski, A., Allerson, C.R., Vasquez, G., Lee, S., Prakash, T.P., Wancewicz, E.V., Witchell, D., Swayze, E.E., 2009. Short antisense oligonucleotides with novel 2′-4′ conformationaly restricted nucleoside analogues show improved potency without increased toxicity in animals. J. Med. Chem. 52, 10–13.

Takahashi, T., Hirano, T., Okada, K., Adachi, M., 2003. Apolipoprotein CIII deficiency prevents the development of hypertriglyceridemia in streptozotocin-induced diabetic mice. Metabolism 52, 1354–1359.

Usui, S., Hara, Y., Hosaki, S., Okazaki, M., 2002. A new on-line dual enzymatic method for simultaneous quantification of cholesterol and triglycerides in lipoproteins by HPLC. J. Lipid Res. 43, 805–814.

Wang, C.S., McConathy, W.J., Kloer, H.U., Alaupovic, P., 1985. Modulation of lipoprotein lipase activity by apolipoproteins. Effect of apolipoprotein C-III. J. Clin. Invest. 75, 384–390.

Yahara, A., Shrestha, A.R., Yamamoto, T., Hari, Y., Osawa, T., Yamaguchi, M., Nishida, M., Kodama, T., Obika, S., 2012. Amido-bridged nucleic acids (AmNAs): synthesis, duplex stability, nuclease resistance, and in vitro antisense potency. Chembiochem 13, 2513–2516.

Yamamoto, T., Harada-Shiba, M., Nakatani, M., Wada, S., Yasuhara, H., Narukawa, K., Sasaki, K., Shibata, M.A., Torigoe, H., Yamaoka, T., Imanishi, T., Obika, S., 2012. Cholesterol-lowering action of BNA-based antisense oligonucleotides targeting PCSK9 in atherogenic diet-induced hypercholesterolemic mice. Mol. Ther. Nucleic Acids 1, e22.

Therapeutic Apheresis and Dialysis

Therapeutic Apheresis and Dialysis 2014; 18(1):93–102
doi: 10.1111/1744-9987.12056

Proteomic Analysis of Proteins Eliminated by Low-Density Lipoprotein Apheresis

Yumiko Yuasa,[1,4] Tsukasa Osaki,[2] Hisashi Makino,[3] Noriyuki Iwamoto,[3] Ichiro Kishimoto,[3] Makoto Usami,[4] Naoto Minamino,[2] and Mariko Harada-Shiba[1]

[1]Department of Molecular Innovation in Lipidology, [2]Department of Molecular Pharmacology, National Cerebral and Cardiovascular Center Research Institute, [3]Department of Endocrinology and Metabolism, National Cerebral and Cardiovascular Center, Osaka and [4]Division of Nutrition and Metabolism, Department of Biophysics, Postgraduate School of Health Science, Kobe University, Kobe, Japan

Abstract: Low-density lipoprotein apheresis (LDL-A) treatment has been shown to decrease serum LDL cholesterol levels and prevent cardiovascular events in homozygous patients with familial hypercholesterolemia. Recently, LDL-A treatment has been suggested to have beneficial effects beyond the removal of LDL particles. In this study, to clarify the preventive effects of LDL-A treatment on atherosclerosis, the waste fluid from the adsorption columns was analyzed. The waste fluid of LDL adsorption columns was analyzed by two-dimensional electrophoresis followed by mass spectrometry. Serum concentrations of the newly identified proteins before and after LDL-A treatment were measured by enzyme-linked immunosorbent assay. We identified 48 kinds of proteins in the waste fluid of LDL adsorption columns, including coagulation factors, thrombogenic factors, complement factors, inflammatory factors and adhesion molecules. In addition to the proteins that were reported to be removed by LDL-A treatment, we newly identified several proteins that have some significant roles in the development of atherosclerosis, including vitronectin and apolipoprotein C-III (Apo C-III). The serum levels of vitronectin and Apo C-III decreased by 82.4% and 54.8%, respectively, after a single LDL-A treatment. While Apo C-III was removed with very low-density lipoprotein (VLDL) and LDL, vitronectin was removed without association with lipoproteins. The removal of proteins observed in the waste fluid has a certain impact on their serum levels, and this may be related to the efficacy of LDL-A treatment. Proteomic analysis of the waste fluid of LDL adsorption columns may provide a rational means of assessing the effects of LDL-A treatment. **Key Words:** Apolipoprotein C-III, Low-density lipoprotein apheresis, Proteomic analysis, Vitronectin.

Familial hypercholesterolemia (FH) is an autosomal-dominant inherited disorder resulting from genetic mutation in the molecules related to low-density lipoprotein receptor (LDLR) pathways (1). Homozygous FH patients show severe symptoms of atherosclerosis such as coronary artery disease (CAD) and valvular heart disease at a young age due to their extremely high levels of serum LDL-cholesterol (LDL-C) from birth (2). Because drugs that act via the upregulation of LDLR activity are not effective in homozygous patients with FH, several attempts have been made to reduce their LDL-C levels and to prevent atherosclerosis. DeGenne et al. conducted plasma exchange (PE) in homozygous FH patients in 1967 (3), and in 1975 Thompson et al. reported the LDL-C-reducing effects of PE on the alleviation of angina pain with the improvement of coronary artery stenosis (4). Subsequently, attempts to remove LDL in more selective ways have been made by using a special double-filtration plasmapheresis (DFPP) method termed thermofiltration (5–7) and an LDL adsorption column (8,9). Collectively, these two methods have been called LDL-apheresis (LDL-A). The use of LDL adsorption columns in particular is selective for LDL removal (8); these columns have been shown to be effective not only for

Received November 2012; revised March 2013.
Address correspondence and reprint requests to Dr Mariko Harada-Shiba, Director, Department of Molecular Innovation in Lipidology, National Cerebral and Cardiovascular Center Research Institute, 5-7-1 Fujishiro-dai, Suita, Osaka 565-8565, Japan. Email: mshiba@ncvc.go.jp

homozygous FH patients but also for severe heterozygous FH patients, as well as for atherosclerotic diseases including arteriosclerosis obliterans (ASO) (10). Although there have been no randomized controlled studies, Mabuchi et al. and Nishimura et al. reported that LDL-A treatment had more beneficial effects, including the prevention of cardiac events and the inhibition of coronary stenosis, compared to treatment with a maximal dose of statins in heterozygous FH patients (11,12).

After the launch of strong statins such as atorvastatin, pitavastatin, and rosuvastatin, some patients on LDL-A treatment withdrew from the therapy because of the high medical costs. However, several patients who withdrew from LDL-A treatment later died of cardiac events, though their serum lipid levels were controlled by a maximal dose of a strong statin at the same level as under LDL-A treatment, as reported by studies from the National Cerebral and Cardiovascular Center and Kanazawa University (13,14). These results suggest that LDL-A treatment can prevent cardiovascular events by removing a series of proteins and substances from the blood in addition to apolipoprotein B (Apo B)-containing lipoproteins. LDL-A treatment using an adsorption column has been reported to reduce Lp(a), fibrinogen; coagulation factors II, V, VII, VIII, X, XI, and XII, serotonin; C-reactive protein (CRP), and amyloid proteins (15,16); while LDL-A treatment using DFPP has been reported to reduce fibrinogen, Lp(a), C3, C4, α_2-macroglobulin, and immunoglobulins (17). These studies were conducted by measuring the target molecules before and after LDL-A treatment. On the basis of the hypothesis that the adsorption column removed atherosclerosis-related proteins other than lipoprotein-binding proteins or positively charged proteins, proteomic analysis of the waste fluid was performed. Edwards et al. reported that proteomics has the potential to reveal proteins that are associated with pathogenesis, by providing a greater understanding of information flow in pathogenic situations (18). Proteomics has been used for analysis of the waste fluid of LDL-A treatment by DFPP, direct adsorption of lipoproteins (DALI), and heparin-mediated extracorporeal LDL precipitation (HELP) (19). However, it has not been applied to analysis of the waste fluid of the dextran sulfate column, which is a major treatment in Japan. In this study, we analyzed stepwise-eluted fluid from LDL adsorption columns by a proteomics approach to identify the proteins removed by the LDL-A treatment and, in turn, to present a possible mechanism underlying the preventive effects of LDL-A treatment on atherosclerosis.

PATIENTS AND METHODS

Patients and LDL-A treatment

The subjects were four FH patients, including one homozygous and three heterozygous patients, who were on regular LDL-A treatment. For LDL-A treatment, MA-03 (Kaneka, Osaka, Japan) and LDL adsorption columns (Liposorber LA-15; Kaneka) were used. The patients' backgrounds are shown in Table 1. All the patients used heparin for anticoagulation for LDL-A treatment, and the treated plasma volumes are shown in Table 1. Each patient gave written informed consent to participate in the study, and the study protocol was endorsed by the ethics committee of the National Cerebral and Cardiovascular Center (approval No. M20-26).

Serological investigation

Blood was collected from the blood removal line immediately before and after LDL-A treatment to determine changes in the levels of lipids, lipoprotein fractions, hematological values, electrolytes, serum proteins, and so on. Vitronectin was determined by the sandwich ELISA method (Human Total Vitronectin ELISA kit; Innovative Research, Novi, MI, USA). The measurements of fibrinogen, D-dimer and apolipoprotein C-III (Apo C-III) were consigned to SRL (Tokyo, Japan) and other items were consigned to the clinical laboratory at our hospital. Lipoprotein fractions were separated by ultracentrifugation. The data are presented as the means ± SEM of three

TABLE 1. *Background of study patients*

Patient No.	Sex (M/F)	Type of FH	HT	DM	Mode of LDL-A treatment			Drug for hypercholesterolemia		
					Duration of LDL-A (year)	Treated plasma volume (mL)	Anticoagulation	Statin	Ezetimibe	Other
1	M	Het.	+	–	2	4000	Heparin	+	+	–
2	M	Hom.	+	–	27	6000	Heparin	+	+	–
3	F	Het.	–	–	16	4000	Heparin	+	–	+
4	M	Het.	+	+	16	4000	Heparin	+	–	+

HT, hypertension; DM, diabetes mellitus; Het., Heterozygote; Hom., Homozygote. (+) Is an affected patient and (–) is a non-affected patient.

measurements in each patient. Comparisons of parameters before and after LDL-A treatment were made by a paired *t*-test using Excel analysis software (Microsoft, Redmond, WA, USA).

Proteomic analysis

Sampling

Three separate samples for proteomic analysis of the waste fluid were obtained twice from the LA-15 system of each patient. Sample 1 was the waste fluid obtained from 0.86 M NaCl solution during LDL-A treatment; Sample 2 was obtained after the removal of lipoproteins by the ultracentrifugation of Sample 1; and Sample 3 was the solution eluted from the column with 2 M NaCl solution.

Sample preparation

Samples 1 to 3 were dialyzed in dialysis buffer, 0.3 mM ethylenediaminetetraacetic acid (EDTA) (pH 7.4), and 0.15 M NaCl using cellulose tubing overnight. After dialysis, Sample 3 was concentrated using a 5 kDa molecular weight cutoff spin concentrator (5 kDa MWCO 4 mL; Agilent Technologies, Santa Clara, CA, USA). Albumin and immunoglobulin in Samples 1 and 2 were removed using an Albumin and IgG Removal kit (GE Healthcare, Chalfont St. Giles, UK).

Isoelectric focusing electrophoresis

Isoelectric focusing electrophoresis was performed using an Immobiline Dry Strip (IPG, pH 3–10, 24 cm, GE Healthcare). Samples 1, 2, and 3 from study patients were each adjusted to a protein concentration of 1 mg/450 μL with the rehydration buffer according to the manual supplied by the manufacturer. The passive hydration of the gels was carried out for 12 h at 20°C, and the isoelectric focusing was performed at 500 V for 1 h, 1000 V for 1 h, 8000 V for 8.2 h, and 500 V for 1 h.

SDS-PAGE

After the isoelectric focusing electrophoresis, the IPG strips were equilibrated in 6 M urea 30% glycerol v/v, 2% sodium dodecyl sulfate (SDS), 50 mM Tris–HCl (pH 8.8), and 0.1% (w/v) dithiothreitol (DTT) for 15 min. Subsequently, the IPG strips were immersed in the above buffer containing 0.25% (w/v) of iodoacetamide instead of DTT at room temperature for 15 min. SDS-polyacrylamide gel electrophoresis (PAGE) was performed using the 12.5% polyacrylamide gel with an Ettan DALT buffer kit (GE Healthcare). Electrophoresis was performed at 4–6 W for 18 h.

Staining and de-staining

After the electrophoresis, the gels were fixed with a fixative solution, 40% methanol (v/v) and 10% acetic acid (v/v), for 30 min and stained in the same mixture containing 0.2% Coomassie Brilliant Blue (CBB) (w/v) for 30 min. The gels were then de-stained with 20% methanol and 5% acetic acid (v/v) solution at room temperature until spots were clearly visible.

In-gel digestion with trypsin

The spots were cut out from the gels, and were further immersed in a solution of 50% acetonitrile (ACN) and 25 mM ammonium hydrogen carbonate. The gel pieces were then dehydrated and dried. Each gel piece was rehydrated with 15 μL of 100 mM ammonium bicarbonate containing 100 μg/mL of trypsin, 7% ACN, and 1% octyl-beta-glucoside and left to stand for 45 min on ice, after which the gel was incubated overnight at 37°C with shaking. An extraction solution containing 50% ACN and 1% trifluoroacetic acid (TFA) was added to the gel and left for 30 min. After centrifugation, the recovered extract was concentrated to 5 to 10 μL using a SpeedVac concentrator (Thermo Scientific, Waltham, MA, USA).

Desalting and condensation by C-tip

Desalting and condensation were performed using a solid phase extraction tip, C-tip (Nikkyo Technos, Tokyo, Japan). After pre-treatment, 5–10 μL of the tryptic digest solution was applied to the tip, washed with 0.1% trifluoroacetic acid (TFA) and 10% ACN, and eluted with a solution of 0.1% TFA and 60% ACN by centrifugation to recover the desalted tryptic digests.

Mass spectrometry (MS) analysis

Tryptic peptides eluted from the C-tip were spotted onto a sample plate (Opti-TOF 384 Well MALDI Plate Inserts; Applied Biosystems, Carlsbad, CA, USA), mixed with a matrix (0.175% alpha-cyano-4-hydroxycinnamic acid, 50% ACN and 0.1% TFA), and air-dried. Each spotted sample was then subjected to mass spectrometric (MS) and tandem mass spectrometric (MS/MS) analysis with a 4800 matrix-assisted laser desorption/ionization time-of-flight/time-of-flight (MALDI TOF/TOF) Analyzer (Applied Biosystems) to identify tryptic peptides. Each spot was analyzed by MS in reflector mode in a mass-to-charge ratio (*m/z*) range of 800 to 4000 (Fig. 1A). MS/MS was performed for digested peptide peaks with a signal-to-noise (S/N) ratio greater than 100 (Fig. 1B). Peak lists were generated by the "Launch Peaks to Mascot" function of the

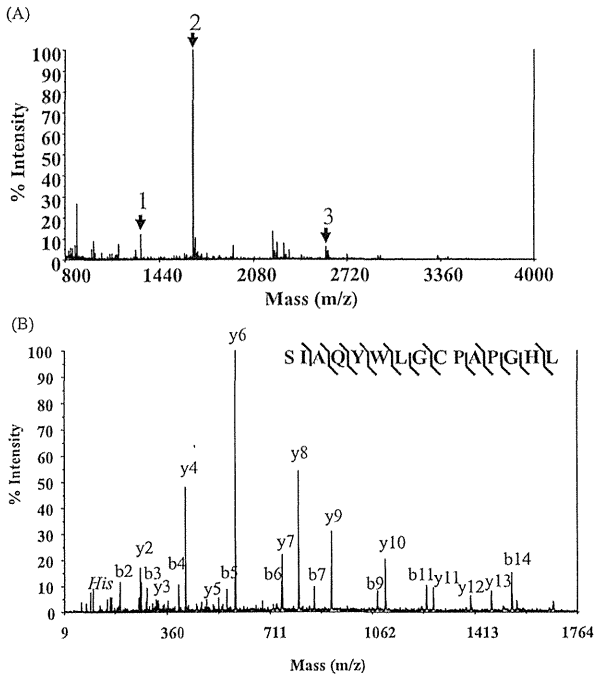

FIG. 1. Peptide mass fingerprint (A) and mass spectrometry/mass spectrometry (MS/MS) spectrum (B) of vitronectin obtained by a 4800 matrix-assisted laser desorption/ionization time-of-flight (MALDI-TOF) analyzer. (A) 1, Vitronectin [453–463], RVDTVDPPYPR; 2, Vitronectin [464–478], SIAQYWLGCPA-PGHL (carbony-tarminal); 3, Vitronectin [422–443], MDWLVPAT-CEPIQSVFFFSGDK. (B) Tryptic peptide number 2 in (A) was identified by nine b-ions and 12 y-ions by MS/MS analysis. *His* shows the ammonium ion of His. The "y" shows the y-ion and the "b" shows the b-ion. The amino acid sequence of the peptide is shown.

4000 Series Explorer software (ver. 3.5; Applied Biosystems). Peak lists were searched against the human NCBInr database (80 128 entries on 18 June 2009) using the Mascot search algorithm (ver. 2.2), with trypsin specification. Carbamide-methylated cysteine was set as a fixed modification. Peptide tolerance was set to 125 ppm, and MS/MS tolerance was 0.4 Da. Peptide sequences with an expectation value lower than 0.05 were identified.

Separation of the lipoprotein and bottom fractions

To determine the removal rate of Apo C-III and vitronectin in the lipoprotein and bottom fractions by LDL-A treatment, the serum was separated by ultracentrifugation ($d < 1.006$: very low-density lipoprotein (VLDL), $1.006 \leq d < 1.019$: intermediate-density lipoprotein (IDL), 1.019d<1.063: LDL, $1.063 \leq d < 1.210$: high-density lipoprotein (HDL), $1.210 < d$: bottom).

RESULTS

Low-density lipoprotein apheresis treatment was performed in one homozygous and three heterozygous patients by using the LDL adsorption method.

Hematologic test and blood chemical analysis data

Hematologic test and blood chemical analysis data before and after LDL-A treatment are shown in Table 2. After a single LDL-A treatment, serum LDL-C levels decreased by 80.9%, total cholesterol

TABLE 2. *Laboratory data before and after a single low-density lipoprotein apheresis treatment*

	Before treatment (Mean ± SD)	After treatment (Mean ± SEM)	Decrease (%)	*P*-value
Total cholesterol (mg/dL)	254 ± 102	73 ± 22	–71.4	**
LDL cholesterol (mg/dL)	194 ± 81	37 ± 19	–80.9	**
HDL cholesterol (mg/dL)	46 ± 22	39 ± 18	–15.4	n.s.
Triglycerides (mg/dL)	132 ± 76	24 ± 16	–81.8	**
Total protein (mg/dL)	7.4 ± 0.6	6.4 ± 0.7	–13.6	**
Albumin (g/dL)	4.6 ± 0.4	4.1 ± 0.5	–12	*
RBC (10×10^5 mm^3)	4.27 ± 0.81	4.52 ± 0.77	5.7	n.s.
WBC (10×10^5 mm^3)	5.8 ± 2.0	7.5 ± 2.5	28.2	n.s.
Hemoglobin (g/dL)	13.4 ± 2.5	13.8 ± 2.6	3	n.s.
Hematocrit (%)	38.5 ± 6.2	40.1 ± 6.4	4.2	n.s.
Plt (10^3/μL)	166 ± 65	152 ± 56	–8.4	n.s.
Na (mEq/L)	138 ± 1	142 ± 1	2.5	**
K (mEq/L)	4.0 ± 0.4	4.1 ± 1	2.5	n.s.
Cl (mEq/L)	104 ± 3	109 ± 4	4.3	n.s.
Ca (mEq/L)	9.6 ± 0.4	9.0 ± 0.3	–5.7	*
Fibrinogen (μg/dL)	203 ± 51	123 ± 31	–39.4	**
D-dimer (μg/mL)	1.04 ± 0.91	1.13 ± 1.013	8.7	n.s.

*$0.01 < P < 0.05$, **$P < 0.01$. HDL, high-density lipoprotein; n.s., not significant; RBC, red blood cell count; SEM, standard error of the mean; WBC, white blood cell count.

(TC) levels by 71.4% and triglyceride (TG) levels by 81.8%, while high-density lipoprotein-cholesterol (HDL-C) showed no significant change. Serum fibrinogen decreased significantly to 39.4%. These results are in good agreement with those previously reported.

Proteomic analysis

The proteomic analysis was performed using three kinds of samples (Sample 1, Sample 2 and Sample 3) from each study patient. Typical two-dimensional gel electrophoresis profiles obtained from a homozygous FH patient (Fig. 2A–C show the data from patient number 2) and from one of three heterozygous FH patients (Fig. 2D–F are the results for patient number 1) are shown. Sample 1, which was prepared from the waste fluid fraction, gave 110 spots (Fig. 2A) and 127 spots (Fig. 2D), while Sample 2, which was prepared by removing lipoproteins from Sample 1, gave 120 (Fig. 2B) and 145 spots (Fig. 2E), in the homozygous and heterozygous patients, respectively. The density and distribution patterns of the protein spots were similar in homozygous and heterozygous patients. Sample 3, the eluate from the column by 2 M NaCl, appeared to yield fewer spots compared to Samples 1 and 2: 30 spots in the homozygous patient (Fig. 2C) and 25 spots in the heterozygous patient (Fig. 2F). Sample 3 also showed similar density and distribution patterns between the homozygous and heterozygous patients.

By mass spectrum analysis of the spots obtained from Samples 1, 2, and 3 of four patients, 48 proteins were identified from 279 spots in Sample 1, 34 proteins from 140 spots in Sample 2, and 10 proteins from 36 spots in Sample 3. As numerous spots gave the same identification results, we identified 48 proteins in total from Samples 1–3 without redundancy. The identified proteins are listed in Table 3. The spots were distributed between 10 kDa and 260 kDa on the gel; the largest was fibronectin and the smallest was Apo C-III. The protein with the lowest pI was vitronectin, and that with the highest was fibrinogen-α-chain (Fig. 3A–C). The identified proteins included coagulation factors such as fibrinogens; antithrombin III; haptoglobin; heparin cofactor; thrombogenic factors such as β_2-glycoprotein I; fibronectin; kininogen I; complement factors; inflammation factors such as Apo C-III and α_1-acid glycoprotein I; and adhesion molecules such as vitronectin. The proteins identified from Sample 3 were mostly fibrinogen α, β, and γ chains; the protein α_1-microglobulin bikunin precursor (AMBP); antithrombin III; and the Ig mu chain C region. Of the proteins identified, β_2-glycoprotein I, clusterin, gelsolin, α_1-antitrypsin, apolipoprotein F (Apo F), CD5 antigen-like, amidase, pigment epithelium-derived factor, tetranectin, transthyretin, vitamin D-binding protein, histidine-rich glycoprotein, alpha-2 HS glycoprotein, and complement component C6 were first found to have been removed by the LDL-adsorption column. Fibrinogen (α, β, and γ chains), antithrombin III apolipoprotein A-I (Apo A-I), and apolipoprotein E (Apo E), which were previously reported to have been removed by LDL-A treatment, were also identified in the waste fluid in this study (Table 3).

Changes in identified protein levels in serum before and after LDL-A treatment

Among the identified proteins, vitronectin, and Apo A-I, A-II, B, C-II, and C-III levels in the serum were measured before and after LDL-A treatment. Vitronectin showed a substantial decrease of 82.4% after a single treatment. In addition, we measured vitronectin levels in the lipoprotein and the bottom fractions before and after LDL-A treatment. Before treatment, the amount of vitronectin in the bottom fraction accounted for 68.8% of the total amount, suggesting that most of the vitronectin was not associated with lipoproteins. After treatment, vitronectin levels were decreased by 83.6% in the bottom fraction and by 43.9% in the lipoprotein fraction. Among apolipoproteins, Apo A-I, A-II, B, C-III, and E decreased significantly after a single treatment. Most of the Apo C-III was found in the lipoprotein fraction, and a negligible amount was seen in the bottom fraction. In addition, Apo C-III levels in the VLDL and LDL fractions decreased by 22.8% and by 42.6% after LDL-A treatment. On the other hand, the amount of Apo C-III in the bottom fraction showed no change, suggesting that Apo C-III was removed in association with VLDL and LDL lipoproteins.

DISCUSSION

The adsorption column used in LDL-A treatment has been reported to remove many proteins, such as fibrinogen, antithrombin III, coagulation factors II, V, VII, VIII, IX, X, XI and XII, CRP, α_1-antitrypsin, serum amyloid A protein, and α_1-acid glycoproteins of inflammation factors and lipoproteins, such as Lp(a), MDA-LDL, sd-LDL, and ox-LDL (15,20,21). On the other hand, DFPP has been reported to remove fibrinogen, Lp(a), C3, C4, β_2-macroglobulin, and immunoglobulins (17). The mechanism of the removal of Apo B-containing lipoproteins is based on the molecular size in DFPP, whereas in the LDL adsorption column, the mechanism is the electrostatic binding to the negatively charged ligand.

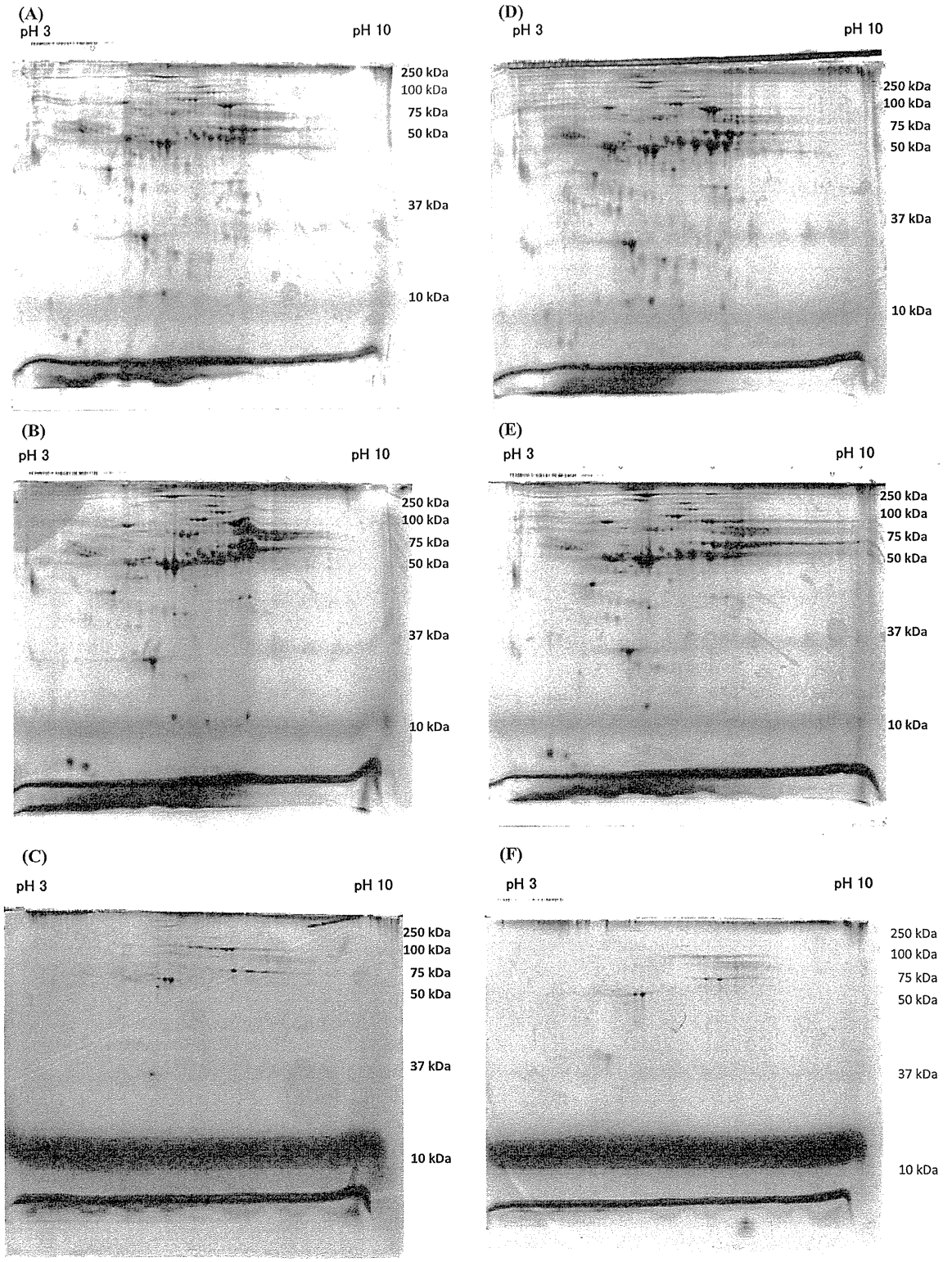

FIG. 2. Two-dimensional gel electrophoresis profiles of the samples prepared from one homozygous familial hypercholesterolemia (FH) patient (A–C) and one heterozygous FH patient (D–F). For each of the two patients, sample 1 (A,D), sample 2 (B,E), and sample 3 (C,F) were subjected to two-dimensional electrophoretic analysis and stained. The horizontal axis/bar shows isoelectric focusing with pH values of 3 to 10, and the vertical axis/bar shows the molecular weight.

TABLE 3. *Identified proteins in the eluate from the low-density lipoprotein apheresis column*

Group	Protein Name	MW	Sample 1	Sample 2	Sample 3
Coagulation factor	α-fibrinogen precursor	69 809	+	+	+
	Antithrombin III	52 618	+	+	+
	β-fibrinogen precursor	54 895	+		
	EGF-containing fibulin-like extracellular Matrix protein 2	49 405	+		
	Fibrinogen γ chain	49 481	+	+	+
	Heparin cofactor II precursor	57 098	+		
	Kininogen I	47 901	+	+	
	β2-glycoprotein I	36 254	+	+	
Thrombogenic factor	Histidine-rich glycoprotein	53 378	+		
	α-1-acid glycoprotein 1 precursor	23 511	+	+	
Inflammation factor	Apolipoprotein C-III	10 822	+	+	
	Inter-alpha-trypsin inhibitor family heavy chain-related protein	103 385	+	+	
	α-1 antitrypsin	46 706	+	+	+
	α-2-glycoprotein 1	34 258	+	+	
	α-2-HS-glycoprotein	39 324	+	+	
Adhesion molecule	Vitronectin	54 335	+	+	
	Fibronectin precursor	256 689	+	+	
Complement component	Complement component C3	187 163	+	+	
	Complement C1r subcomponent	80 173	+		
	Complement component C4A	192 861	+	+	
	Complement factor B	85 562	+	+	+
	Complement factor C6	104 843	+		
	C1-inhibitor	32 708	+		
	Complement C1s	37 208	+		
	Complement component C6	104 786	+		
Glycoproteins	α-1B-glycoprotein	54 254	+	+	
	Angiotensinogen	53 154	+		
	Clusterin	52 495	+	+	
	Hemopexin	51 676	+	+	
	Zinc-alpha-2-glycoprotein	34 259	+	+	
Apolipoproteins	Apolipoprotein A-I	30 778	+	+	+
	Apolipoprotein A-IV	45 399	+	+	
	Apolipoprotein C-II	11 284	+	+	
	Apolipoprotein E	36 154	+	+	
	Apolipoprotein F	35 399	+		
Immunogloblin	Ig kappa chain C region	11 609	+	+	
	Ig mu chain C region	49 307	+		
Others	CD5 antigen-like	38 088	+	+	
	Gelsolin	85 698	+	+	+
	N-acetylmuramoyl-L-alanine amidase	62 217	+		
	Pigment epithelium-derived factor	46 312	+	+	+
	Protein AMBP	38 999	+	+	
	Retinol-binding protein 4	23 010	+	+	
	Serotransferrin	77 064	+	+	+
	Serum albumin	69 367	+		
	Tetranectin	22 566	+	+	+
	Transthyretin	20 193	+	+	
	Vitamin D-binding protein	52 964	+	+	

(+) Protein was identified in the waste fluid and eluted solution from the adsorption column.

Therefore, the proteins removed by DFPP may be associated with VLDL and/or LDL. On the other hand, the removal of proteins by the LDL adsorption column has three mechanisms, association with VLDL and/or LDL, electrostatic binding of their positive charge to the ligands, or nonspecific binding to the column.

Dihazi et al. reported the clearance of proteins by three kinds of LDL-A methods: DFPP, DALI, and HELP (19). They reported that 74 proteins were identified and, among these, 15 proteins, that is, α-1 antitrypsin, α-2 antiplasmin, fibrinogen A alpha polypeptide, fibrinogen beta chain, fibrinogen gamma polypeptide, kininogen I, transthyretin, alpha-2-macroglobulin, complement C4 precursor, complement C3, complement component C4B, complement factor H –precursor, haptoglobin, Ig kappa chain C region and immunoglobulin J chain, were reported to be removed by all three methods. In our study, 48 proteins were found to be removed by the LDL adsorption columns, and among them, eight proteins, β-fibrinogen precursor, fibrinogen γ chain, kininogen

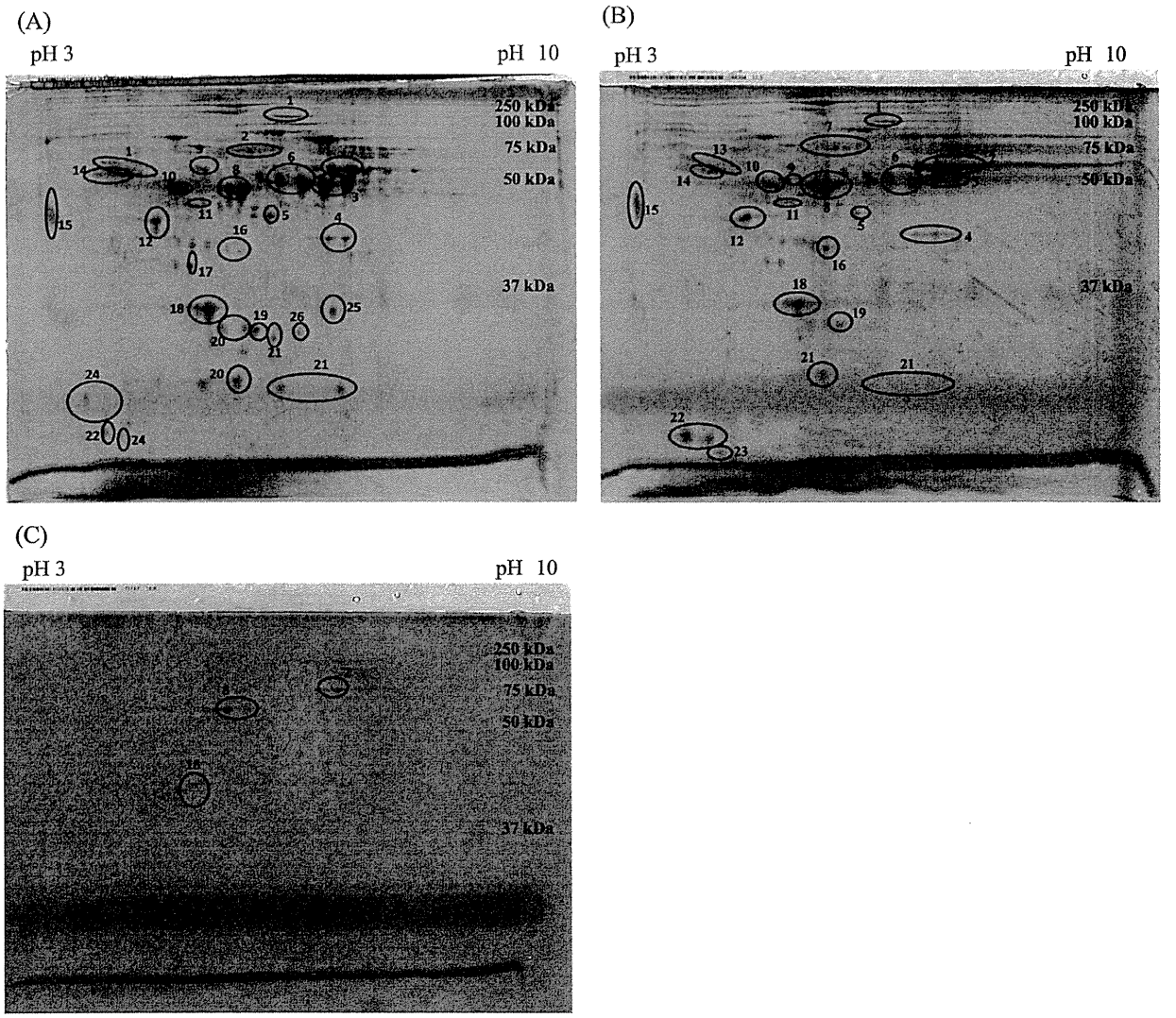

FIG. 3. Protein spot map on two-dimensional gel electrophoresis. Each spot was excised from the gel and subjected to in-gel trypsin digestion, followed by matrix-assisted laser desorption/ionization time-of-flight (MALDI-TOF) mass spectrometry/mass spectrometry (MS/MS) analysis. (1) Fibronectin, (2) β_2 glycoprotein I, (3) fibrinogen β-chain, (4) complement factor CA4, (5) complement factor H, (6) apolipoprotein H, (7) hemopexin, (8) fibrinogen γ-chain, (9) vitamin D-binding protein, (10) α_1 antitrypsin, (11) apolipoprotein A-IV, (12) complement factor 3, (13) kininogen I, (14) α-HS glycoprotein, (15) vitronectin, (16) apolipoprotein E, (17) microglobulin binding protein, (18) apolipoprotein A-I, (19) haptoglobin, (20) transthyretin, (21) fibrinogen α-chain precursor, (22) apolipoprotein C-III, (23) apolipoprotein C-II, (24) vitronectin.

I, α-1 antitrypsin, fibronectin precursor, complement component C3, Ig kappa chain C region and transthyretin, were the proteins removed by all four methods—that is, HELP, DFPP, DALI and LDL adsorption—although the analytical methods were not the same. There have been no data on long-term clinical outcomes indicating that one of the existing lipid apheresis methods is superior to any of the others. Indeed, the report of Dihazi that analyzed the proteins removed by each LDL-A method does not support the superiority of any specific method. The fact that fibronectin and fibrinogen were removed by all four methods is of interest, because removal of these proteins has been reported to lower plasma viscosity which has been related to a significant improvement of peripheral flow.

Proteins that have heparin-binding domains, such as fibrinogen, antithrombin III, fibronectin, and α_1-β-glycoprotein, carry positive charges, which may be removed by ionic interaction. Apolipoproteins known as lipoprotein-associated proteins may be removed together with the lipoproteins. We identified not only proteins reported to be removed by LDL-A treatment (10,21,22), but also new molecules such

as vitronectin and Apo C-III, which are known to have important roles in atherogenesis. It is of interest that while vitronection was not removed with Apo B-containing lipoproteins but by ionic interaction, Apo C-III was removed with Apo B-containing lipoproteins. We also found that the serum levels of Apo C-III and vitronectin were significantly decreased after a single LDL-A treatment.

Vitronectin is a heparin-binding protein with a molecular weight of 54 kDa, 5.55 pI, and is contained at 200 to 400 μg/mL in human serum. Vitronectin carries positive charges in the heparin binding domain, suggesting that its binding mechanism to the negative charges of dextran sulfate is plausible. Serum vitronectin levels are reportedly increased in patients with significant stenosis in two or more segments of the coronary arteries compared to those with stenosis in no or only one segment (23). Peng et al. reported that vitronectin-knockout mice show reduced neointima formation after carotid injury ligation or chemical injury compared with wild-type mice (24). Although vitronectin does not directly change vascular smooth muscle cell (VSMC) proliferation, this protein was reported to promote neointima development by enhancing VSMC migration. Vitronectin reduction may be one of the beneficial effects of LDL-A treatment in the prevention of atherosclerosis.

Apo C-III is 10 kDa in molecular weight and 5.23 in pI, and is contained at 5.4 mg/dL to 10.0 mg/dL in human serum. Apo C-III is known to be distributed mainly in VLDL and HDL, and secreted as a component of VLDL from the liver (25). The physiological role of Apo C-III is the regulation of lipolysis through noncompetitive inhibition of endothelial cell-bound LPL that hydrolyzes TG in VLDL, transforming large TG-rich particles into smaller TG-depleted remnant lipoproteins (25). In several clinical studies, higher Apo C-III levels were associated with an increased severity of CVD in patients with angiographically defined coronary artery diseases (25). Pollin et al. reported that Lancaster Amish patients are heterozygous carriers of a null mutation in the gene encoding Apo C-III, and thus express half the amount of Apo C-III present in noncarriers. The carriers had higher HDL-C levels, lower TC and LDL-C levels (26), and less detectable coronary artery calcification than noncarriers (26). Null mutation in Apo C-III confers favorable lipid profiles and apparent cardioprotection without any obvious detrimental effect; this raised the possibility that therapies targeting Apo C-III would be clinically effective in reducing cardiovascular events (26). In our study, Apo C-III was decreased by 54.8% with a single LDL-A treatment. Moreover, the Apo C-III level in VLDL was decreased by 77.2%. This suggests that the decrease in Apo C-III by LDL-A treatment is one of the protective effects against cardiovascular disease.

There are some limitations to this study. First, some proteins that LDL-A treatment removes have beneficial effects on the inhibition of atherosclerosis development. Second, some proteins having physiological importance, such as immunoglobulin, albumin, transthyretin and so on, were removed by the adsorption column. In order to evaluate the effect of removal of each protein by LDL-apheresis, a comprehensive understanding of each factor involved in the pathogenesis and pathophysiology based on the analysis of both patients and animal models will be needed.

CONCLUSION

In this study, several proteins that might be involved in the cause and pathophysiology of atherosclerosis were identified in the waste fluid of lipoprotein apheresis treatment by proteomic analysis. Proteomic analysis may provide information on the mechanisms underlying the effects of LDL-A treatment on atherosclerosis, and also could provide data to broaden the application of the treatment, thus demonstrating this treatment's usefulness from these additional perspectives.

Acknowledgments: This work was supported by Grants-in-Aid for Scientific Research from the Japanese Ministry of Health, Labor, and Welfare (H23-seisaku tansaku-ippan-004 and H23-nanji-ippan-011) and the Cardiovascular Research Foundation (Suita, Japan). The authors thank Ms Mika Nishimura, Ms Eiko Shibata, Ms Mai Inoue, and Ms Megumu Morimoto of the Department of Molecular Innovation in Lipidology, National Cerebral and Cardiovascular Center Research Institute for their support and advice. We also thank Mr Teruyuki Hayashi, Mr Takayuki Nishigaki, Mr Kohji Ogawa, and the clinical engineers of the Department of Clinical Engineering, National Cerebral and Cardiovascular Center for their technical support.

REFERENCES

1. Goldstein JL, Hobbs HH, Brown MS. Familial hypercholesterolemia. In: Scriver CR, Beaudet A, Sly WS, Valle D, eds. *The Metabolic and Molecular Bases of Inherited Disease* 8th edn. New York: McGraw-Hil, 2001; 2863–2913.
2. Makino H, Harada-Shiba M. Long-term effect of low-density lipoprotein apheresis in patients with homozygous familial hypercholesterolemia. *Ther Apher Dial* 2003;7:397–401.
3. de Gennes JL, Touraine R, Maunand B, Truffert J, Laudat P. [Homozygous cutaneo-tendinous forms of hypercholesteremic xanthomatosis in an exemplary familial case. Trial of plasmapheresis ans heroic treatment]. *Bull Mem Soc Med Hop Paris* 1967;118:1377–402.

4. Thompson GR, Lowenthal R, Myant NB. Plasma exchange in the management of homozygous familial hypercholesterolaemia. *Lancet* 1975;1:1208–11.
5. Mineshima M, Agishi T, Hasuo Y, Kaneko I, Era K, Ota K. Effect of membrane trapping in plasma fractionator on separative characteristics. *Int J Artif Organs* 1988;11:191–4.
6. Usami M, Horiuchi T, Emura M et al. Thermal effect of LDL/HDL separation in membrane filtration; thermofiltration. *Trans Am Soc Artif Intern Organs* 1985;31:716–21.
7. Nosé Y, Usami M, Malchesky PS et al. Clinical thermofiltration: initial application. *Artif Organs* 1985;9:425–7.
8. Tani N. Development of selective low-density lipoprotein (LDL) apheresis system: immobilized polyanion as LDL-specific adsorption for LDL apheresis system. 1996. *Ther Apher* 2000;4:135–41.
9. Yokoyama S, Hayashi R, Satani M, Yamamoto A. Selective removal of low density lipoprotein by plasmapheresis in familial hypercholesterolemia. *Arteriosclerosis* 1985;5:613–22.
10. Kobayashi S, Oka M, Moriya H, Maesato K, Okamoto K, Ohtake T. LDL-apheresis reduces P-Selectin, CRP and fibrinogen—possible important implications for improving atherosclerosis. *Ther Apher Dial* 2006;10:219–23.
11. Mabuchi H, Koizumi J, Shimizu M et al. Long-term efficacy of low-density lipoprotein apheresis on coronary heart disease in familial hypercholesterolemia. Hokuriku-FH-LDL-Apheresis Study Group. *Am J Cardiol* 1998;82:1489–95.
12. Nishimura S, Sekiguchi M, Kano T et al. Effects of intensive lipid lowering by low-density lipoprotein apheresis on regression of coronary atherosclerosis in patients with familial hypercholesterolemia: Japan Low-density Lipoprotein Apheresis Coronary Atherosclerosis Prospective Study (L-CAPS). *Atherosclerosis* 1999;144:409–17.
13. Takata M, Kawashiri M, Yamagishi M, Mabuchi H. Study on prognosis of patients with familal hypercholesterolemia (FH) who have withdrawn from LDL apheresis. *Lipid* 2007;18:86–90.
14. Harada-Shiba M, Nakahama H, Nagumo S et al. Long-term prognosis of LDL-apheresis in homozygous and heterozygous familial hypercholesterolemia. *Jpn J Apher* 2006;25:65.
15. Kojima S, Harada-Shiba M, Toyota Y et al. Changes in coagulation factors by passage through a dextran sulfate cellulose column during low-density lipoprotein apheresis. *Int J Artif Organs* 1992;15:185–90.
16. Cucuianu M, Dican L. Coagulation factor XIII and atherothrombosis. A mini-review. *Rom J Intern Med* 2003;41:339–55.
17. Klingel R, Fassbender T, Fassbender C, Gohlen B. From membrane differential filtration to lipidfiltration: technological progress in low-density lipoprotein apheresis. *Ther Apher Dial* 2003;7:350–8.
18. Edwards AV, White MY, Cordwell SJ. The role of proteomics in clinical cardiovascular biomarker discovery. *Mol Cell Proteomics* 2008;7:1824–37.
19. Dihazi H, Koziolek MJ, Sollner T et al. Protein adsorption during LDL-apheresis: proteomic analysis. *Nephrol Dial Transplant* 2008;23:2925–35.
20. Kojima S, Harada-Shiba M, Yamamoto A. Plasma constituents other than low-density lipoprotein adsorbed by dextran-sulfate column. *Ther Apher* 1997;1:309–13.
21. Knisel W, Di Nicuolo A, Pfohl M et al. Different effects of two methods of low-density lipoprotein apheresis on the coagulation and fibrinolytic systems. *J Intern Med* 1993;234:479–87.
22. Mabuchi H, Michishita I, Takeda M et al. A new low density lipoprotein apheresis system using two dextran sulfate cellulose columns in an automated column regenerating unit (LDL continuous apheresis). *Atherosclerosis* 1987;68:19–25.
23. Ekmekci OB, Ekmekci H. Vitronectin in atherosclerotic disease. *Clin Chim Acta* 2006;368:77–83.
24. Peng L, Bhatia N, Parker AC, Zhu Y, Fay WP. Endogenous vitronectin and plasminogen activator inhibitor-1 promote neointima formation in murine carotid arteries. *Arterioscler Thromb Vasc Biol* 2002;22:934–9.
25. Ooi EM, Barrett PH, Chan DC, Watts GF. Apolipoprotein C-III: understanding an emerging cardiovascular risk factor. *Clin Sci (Lond)* 2008;114:611–24.
26. Pollin TI, Damcott CM, Shen H et al. A null mutation in human APOC3 confers a favorable plasma lipid profile and apparent cardioprotection. *Science* 2008;322:1702–5.

Bioorganic & Medicinal Chemistry 23 (2015) 33–37

Contents lists available at ScienceDirect

Bioorganic & Medicinal Chemistry

journal homepage: www.elsevier.com/locate/bmc

Synthesis and hybridization property of a boat-shaped pyranosyl nucleic acid containing an exocyclic methylene group in the sugar moiety

Kazuto Mori [a], Tetsuya Kodama [b,*], Satoshi Obika [a,*]

[a] Graduate School of Pharmaceutical Sciences, Osaka University, 1-6 Yamadaoka, Suita, Osaka 565-0871, Japan
[b] Graduate School of Pharmaceutical Sciences, Nagoya University, Furo-cho, Chikusa-ku, Nagoya, Aichi 464-8601, Japan

ARTICLE INFO

Article history:
Received 6 November 2014
Revised 19 November 2014
Accepted 20 November 2014
Available online 28 November 2014

Keywords:
Nucleic acids
Carbohydrates
Oligonucleotides

ABSTRACT

A boat-shaped pyranosyl nucleic acid (BsNA) having an exocyclic methylene group in the sugar moiety was synthesized to investigate the possibility that the axial H3′ of original BsNA is the cause of its duplex destabilization. The synthesized BsNA analog was chemically stable against various nucleophiles. From the thermal stability of duplex oligonucleotides including the BsNA analog, it was found that the duplex-forming ability can be sensitive to the size of functional groups at the 3′-position.

1. Introduction

Many conformationally restricted nucleotides have been developed to date.[1] Especially, 2′,4′-bridged nucleic acid (2′,4′-BNA)[2]/locked nucleic acid (LNA)[3] developed independently by our group and Wengel's group is used in therapeutic application[4] and nanotechnology[5] because of its high affinity with complementary single stranded DNA and RNA (ssDNA, ssRNA). Its outstanding duplex-forming ability is derived from the preorganized sugar conformation that mimics a nucleotide in an A-type RNA duplex. Although various 2′,4′-BNA/LNA analogs have been developed in the past,[1] few analogs[6] have higher binding affinities for complementary strands than that of original 2′,4′-BNA/LNA. In addition, 2′,4′-BNA^{COC}, whose sugar conformation is closest to a typical A-type RNA duplex in the 2′,4′-BNA/LNA analogs, does not have the highest duplex-forming ability.[7] Hence, it is necessary to develop a novel type of artificial nucleic acid on the basis of new strategy.

Recently, we designed and synthesized a boat-shaped glucopyranosyl nucleic acid (BsNA) **1**,[8] which had a constrained pyranose as the basic skeleton (Fig. 1). Regrettably, the incorporation of BsNA **1**-T into oligonucleotides decreased the duplex-forming ability with a complementary ssDNA and ssRNA. Some factors can be attributed to this destabilization. One is the axial H3′ which can invade between neighboring nucleobases and inhibit π–π stacking interaction (Fig. 2a). Pedersen's group reported 3′-methoxy locked pyranosyl nucleic acid (LpNA)[9] (Fig. 1), which had a low binding

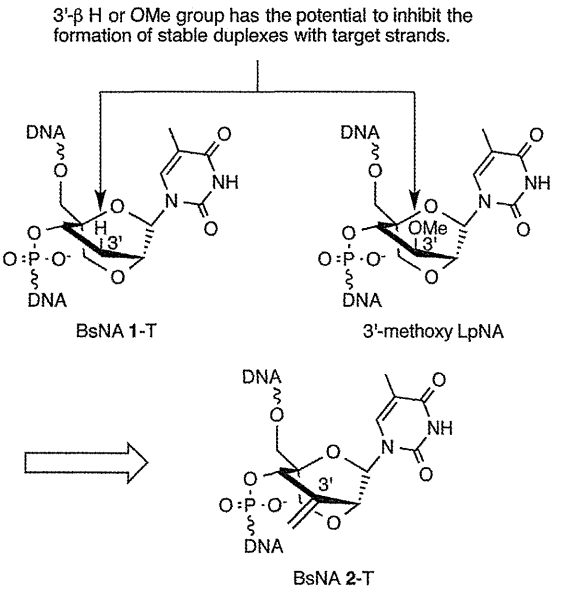

Figure 1. The structure of BsNA **1**-T and 3′-methoxy LpNA and design of BsNA **2**-T.

* Corresponding authors. Tel./fax: +81 5 2789 2971 (T.K.); tel.: +81 6 6879 8200; fax: +81 6 6879 8204 (S.O.).
E-mail addresses: kodama@ps.nagoya-u.ac.jp (T. Kodama), obika@phs.osaka-u.ac.jp (S. Obika).

http://dx.doi.org/10.1016/j.bmc.2014.11.030
0968-0896/

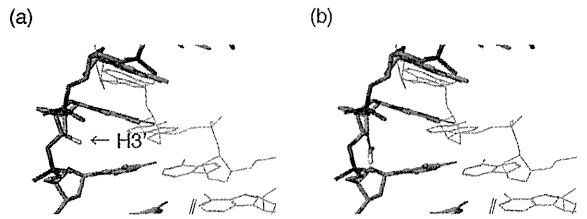

Figure 2. Representative low energy structure of an A-type DNA duplex comprising BsNA **1** (a) and the structure with an exocyclic methylene group (BsNA **2**) modeled into the sugar moiety (b).

affinity with complementary strands as with the case of BsNA **1**. They also suggested that the axial position of the C3′-OMe group can cause a destabilization of a duplex.

In this study, we newly designed and synthesized a BsNA analog that does not have the axial substituent at 3′-position. At first, replacing the C3′ with oxygen atom was occurred to us, but it takes a great deal of exertion to synthesize that analog owing to its own acetal structure.[10] Therefore, we decided to introduce an exocyclic methylene group to the C3′ position to eliminate the axial H3′ (Fig. 1). Recently, Seth's group also reported that an exocyclic methylene group could act as a bioisostere of the 2′-oxygene atom in 2′,4′-BNA/LNA.[6a] Since BsNA **2**-T has no functional groups at the axial C3′ position (Fig. 2b), the duplex forming ability will be improved if the axial H3′ is the cause of the duplex destabilization.

2. Results and discussion

2.1. Synthesis of BsNA 2

BsNA **2**-T was synthesized from known glucopyranoside **3**[8a] as shown in Scheme 1. First, glucopyranoside **3** was deacetylated to give triol **4**. When glucopyranoside **3** was reacted with K_2CO_3 and MeOH, the reaction yield was very low because of the elimination of the tosylate group. This problem was negligible when **3** was treated with methylamine at 0 °C, and desired triol **4** was obtained at high yield. Next, the 4′- and 6′-hydroxy groups of triol **4** were protected as a isopropylidene acetal, and the resulting compound **5** was subjected to sodium hydride under moderate heating conditions to form the bridge between the C2′- and C5′-positions.

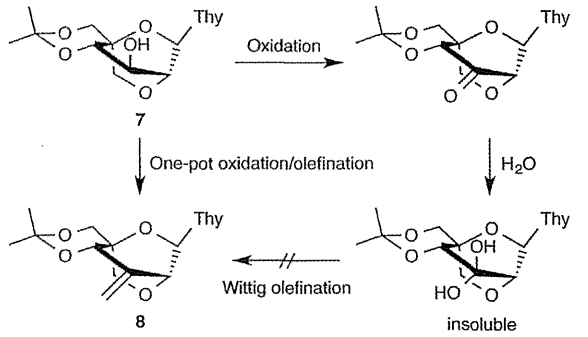

Figure 3. The reason for adopting one-pot oxidation/olefination procedure to obtain alkene **8**.

Subsequently, the resultant compound **6** was exposed to hydrogenolysis conditions using palladium hydroxide to remove benzyl group. When alcohol **7** was oxidized, the resultant ketone was easily hydrated under an air atmosphere. The desired alkene **8** was not yielded from the hydrated compound using Wittig reagent (Fig. 3). Once the hydrate generated, it exhibited an insoluble property and the removal of water from the hydrate was difficult by typical dehydration procedures. Therefore, one-pot oxidation/olefination procedure was adopted. Alcohol **7** was firstly oxidized using PDC, and then methyl triphenyl phosphonium ylide was added to the reaction mixture to afford alkene **8**. Next, removal of the isopropylidene group with aqueous acetic acid furnished nucleoside **9**. Finally, tritylation of **9** at the 6′-hydroxy group with 4,4′-dimethoxytrityl chloride (DMTrCl) and phosphitylation at the 4′-hydroxy group of **10** with 2-cyanoethyl *N*,*N*-diisopropylaminochlorophosphoramidite afforded the desired phosphoramidite building block **11**.

Phosphoramidite **11** was introduced into oligodeoxynucleotide (ODN) using an automated DNA synthesizer. The sequence was the same as that of our previous work.[8a] The concentration of phosphoramidite **11** was 0.1 M and the coupling time was prolonged to 8 min. 5-[3,5-Bis(trifluoromethyl)phenyl]-1*H*-tetrazole was used as an activator. Coupling yields were checked by trityl monitoring and were estimated to be over 95%. Synthesized ODN was cleaved from the solid support and deprotected by treatment with ammonium hydroxide solution. The obtained ODN **12** was purified by

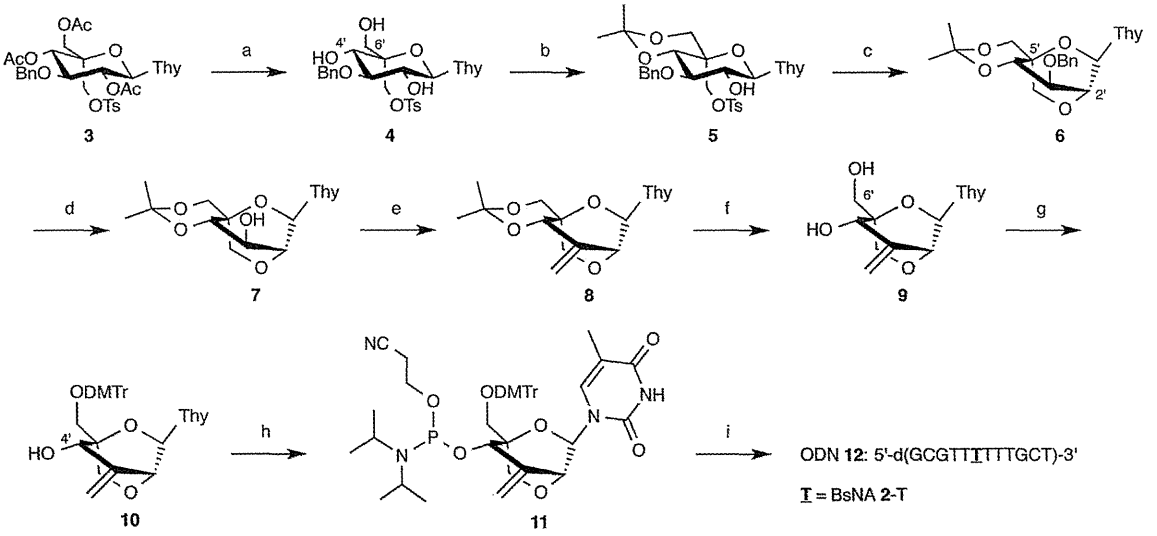

Scheme 1. Reagents and conditions: (a) 40% aq CH_3NH_2, THF, 0 °C, 95%; (b) 2,2-dimethoxypropane, CSA, DMF, rt, 88%; (c) NaH, DMF, 60 °C, 97%; (d) H_2, $Pd(OH)_2$/C, AcOEt, rt, 94%; (e) PDC, MS4A, CH_2Cl_2, rt, then Ph_3PCH_3Br, *n*-BuLi, THF, rt, 61%; (f) 60% aq AcOH, rt, 93%; (g) DMTrCl, pyridine, rt, 96%; (h) 2-cyanoethyl *N*,*N*-diisopropylchlorophosphoramidite, *N*,*N*-diisopropylethylamine, CH_3CN, 0 °C, 79%; (i) DNA synthesis. Thy = thymin-1-yl.

Table 1
Evaluation of thermal denaturation temperatures (T_m values) of duplexes[a]

Oligodeoxynucleotides[b]	DNA complement		RNA complement	
	T_m (°C)	ΔT_m[c]	T_m (°C)	ΔT_m[c]
Natural	51	–	47	–
5′-d(GCGTT**T**TTTGCT)-3′ (**12**)	33	−18	31	−16
5′-d(GCGTTTTTTGCT)-3′ (**13**)	41	−10	39	−8

[a] Target strand sequence: 5′-AGCAAAAAACGC-3′. Thermal denaturation studies' conditions: 10 mM sodium phosphate buffer (pH 7.2) containing 100 mM NaCl; each strand concentration = 4 μM; scan rate of 0.5 °C min^{-1} at 260 nm. T_m was determined by taking the first derivative of the melting curve. The number is the average of three independent measurements.
[b] **T** = BsNA **2**-T, *T* = BsNA **1**-T.
[c] ΔT_ms are calculated relative to T_m values of unmodified DNA–DNA and DNA–RNA duplexes.

reverse-phase HPLC and characterized by MALDI-TOF mass spectrometry.

2.2. Chemical stability of BsNA 2

BsNA **2** has a reactive allylphosphate ester which could be cleaved by nucleophiles.[11] This structure is described as an important feature in the biological activity of some nucleoside antibiotics[12] or antineoplastic agent[13] possibly due to enhanced chemical reactivity. Therefore, there was concern that the 3′ oxygen atom was eliminated during the deprotection process of ODN synthesis using ammonium hydroxide. However, such a cleaved ODN fragment was not observed and BsNA **2** proved to be stable against amines. We evaluated its chemical stability in some detail. Figure S1 shows the reverse-phase HPLC profile of the mixture after treatment of ODN **12** with 1 mM glutathione and 10 mM $MgCl_2$ for 12 h. The peak corresponding to ODN **12** did not disappeared, and the notable new peak derived from the ODN was not observed. As a result, BsNA **2** was stable on the conditions that it was heated or treated with thiol and divalent metal ion, and the worrying strand-breakage was not occurred.

2.3. Evaluation of duplex-forming ability of BsNA 2

We evaluated the affinity of the synthesized ODN with complementary ssDNA and ssRNA through UV melting experiments. The UV melting profiles are shown in Figures S2 and S3, and the thermal denaturation temperatures (T_m values) are summarized in Table 1. ODN **12** did not improve the thermal stabilities of the duplexes with ssDNA and ssRNA (ΔT_m = −18, −16); indeed, the duplex forming ability of ODN **12** was still lower than that of ODN **13**. This additional destabilization can be explained by a steric clash between the introduced exocyclic methylene group and the neighboring nucleotide which reduced π–π stacking in a different way from that of BsNA **1**. It was reported that an exocyclic methylene group can be sterically hindered in the hybridization when it is located in the major groove of the duplex.[14] The C3′-exocyclic methylene group of BsNA **2** might act in that manner.

Given the fact that the introduction of the exocyclic methylene group to the C3′ position lead to the further decrease of the binding affinity of BsNA **1**, one could anticipate that the binding affinity is sensitive to the size of functional groups at the 3′-position and will be improved when replacing the C3′ with smaller groups. However, it should be noted that the duplex-forming ability of BsNAs is too lower than is assumed based on the past report[14] and other factors, for example, the nucleobase lean and the nucleobase orientation, may be attributed to the destabilization of the duplexes. It is difficult to make conclusions about the factor affecting the binding affinity of BsNAs and the investigation of the above hypotheses is still in progress.

3. Conclusion

We successfully synthesized a BsNA analog bearing an exocyclic methylene group in the sugar moiety. The synthesized BsNA analog was chemically stable. The binding affinity of the analog with ssDNA and ssRNA was still lower than that of original BsNA possibly due to a steric clash between the introduced exocyclic methylene group and the neighboring nucleotide. Therefore, it is expected that the duplex-forming ability is sensitive to the size of functional groups at 3′-position and replacing the C3′ with smaller groups will lead to an improvement of it. However, other structural properties cannot be ruled out as the cause of the duplex destabilization and the investigation of these hypotheses is currently underway in our laboratory.

4. Experimental

4.1. General

Dichloromethane, DMF and pyridine were distilled from CaH_2 and the other reagents used as received from commercial suppliers. ^1H NMR (400 and 300 MHz), ^{13}C NMR (100.5 and 75.5 MHz) and ^{31}P NMR (161.8 MHz) were recorded on JEOL JNM-ECS-400 or JNM-ECS-300 spectrometers. Chemical shifts are reported in parts per million referenced to internal tetramethylsilane (0.00 ppm), residual $CHCl_3$ (7.26 ppm), CH_3CN (1.94 ppm), or DMSO (2.50 ppm) for ^1H NMR, and chloroform-d_1 (77.16 ppm) or acetonitrile-d_3 (118.26 ppm) for ^{13}C NMR. Relative to 85% H_3PO_4 as external standard for ^{31}P NMR. IR spectra were recorded on a JASCO FT/IR-4200 spectrometers. Optical rotations were recorded on a JASCO DIP-370 instrument. Mass spectra were measured on JEOL JMS-600 or JMS-700 mass spectrometers. MALDI-TOF mass spectra were recorded on a Bruker Daltonics Autoflex II TOF/TOF mass spectrometer. For column chromatography, Fuji Silysia PSQ-100B or FL-100D silica gel was used. For high performance liquid chromatography (HPLC), SHIMADZU LC-6AD, SPD-10AV_{VP} and CTO-10A_{VP} were used. Thermal denaturation experiments were carried out on SHIMADZU UV-1650 and UV-1800 spectrometers equipped with a T_m analysis accessory.

4.2. 1-{3-*O*-Benzyl-5-*C*-(tosyloxymethyl)-β-D-glucopyranosyl}thymine 4

To a solution of compound **3** (689 mg, 1.0 mmol) in THF (10 mL) was added aqueous 40% methylamine (4.2 mL, 50 mmol) at 0 °C and the resultant mixture was stirred at 0 °C for 7 h. Further aqueous 40% methylamine (1.7 mL, 20 mmol) was added to the mixture and the mixture was stirred at 0 °C for 4 h. Again, aqueous 40% methylamine (0.8 mL, 10 mmol) was added to the mixture and the mixture was stirred at 0 °C for 2 h. After removal of THF under reduced pressure, the mixture was separated with H_2O and AcOEt and the aqueous layer was extracted with AcOEt. The combined organic layer was dried over Na_2SO_4, and concentered. The crude product was purified by column chromatography (SiO_2, *n*-hexane/AcOEt = 1:5) to give compound **4** (535 mg, 95%) as a white foam. $[\alpha]_D^{22}$ −13.4 (*c* 1.00, CH_3OH); IR ν_{max} (KBr): 1691, 3332 cm^{-1}; ^1H NMR (400 MHz, CD_3CN) δ 1.84 (3H, d, *J* = 1 Hz), 2.44 (3H, s), 3.07 (1H, br s), 3.42 (1H, d, *J* = 12 Hz), 3.52 (1H, d, *J* = 12 Hz), 3.60–3.87 (5H, m), 4.06 (1H, d, *J* = 11 Hz), 4.45 (1H, d, *J* = 11 Hz), 4.72 (1H, d, *J* = 11 Hz), 4.84 (1H, d, *J* = 11 Hz), 5.86 (1H, d, *J* = 9 Hz), 7.27–7.45 (8H, m), 7.83 (2H, d, *J* = 9 Hz), 9.24 (1H, br s); ^{13}C NMR (100.5 MHz, CD_3CN) δ 2.4, 21.6, 64.1, 68.6, 71.2, 72.8, 75.5, 79.8, 80.2, 82.4, 111.6, 128.3, 128.7, 128.9, 129.1, 131.0, 132.9, 137.0, 140.0, 146.6, 151.7, 164.4; MS (EI) *m/z* (I_{rel},%) 562 (0.1), 480 (1.0), 390 (5.2), 264 (4.4), 172 (6.0), 91 (100), 65

(10.8); HRMS (EI): Calcd for $C_{26}H_{30}N_2O_{10}S$ $[M]^+$: 562.1621. Found: 562.1643.

4.3. 1-{3-*O*-Benzyl-4,6-*O*-isopropylidene-5-*C*-(tosyloxymethyl)-β-D-glucopyranosyl}thymine 5

To a solution of compound **4** (514 mg, 0.91 mmol) in DMF (9.1 mL) were added 2,2-dimethoxypropane (1.1 mL, 9.1 mmol) and (+)-10-camphorsulfonic acid (21 mg, 0.09 mmol) and the resultant mixture was stirred at room temperature for 13 h under a N_2 atmosphere. Further 2,2-dimethoxypropane (0.2 mL, 1.8 mmol) was added to the mixture and the mixture was stirred at room temperature for 2 h. After addition of saturated aq $NaHCO_3$, the reaction mixture was extracted with AcOEt, the organic layer was dried over Na_2SO_4, and concentered. The crude product was purified by column chromatography (SiO_2, *n*-hexane/AcOEt = 2:5) to give compound **5** (481 mg, 88%) as a white foam. $[\alpha]_D^{22}$ −2.6 (*c* 1.00, $CHCl_3$); IR ν_{max} (KBr): 1598, 1704, 2992, 3221 cm^{-1}; ^1H NMR (400 MHz, $CDCl_3$) δ 1.31 (3H, s), 1.46 (3H, s), 1.86 (3H, s), 2.41 (3H, s), 3.60 (1H, d, *J* = 11 Hz), 3.78–3.91 (4H, m), 4.03 (1H, br s), 4.55 (1H, d, *J* = 11 Hz), 4.69 (1H, d, *J* = 11 Hz), 4.75 (1H, d, *J* = 11 Hz), 4.81 (1H, d, *J* = 11 Hz), 5.97 (1H, d, *J* = 9 Hz), 7.08 (1H, s), 7.24–7.33 (7H, m), 7.83 (2H, d, *J* = 8 Hz), 9.35 (1H, br s); ^{13}C NMR (100.5 MHz, CD_3CN) δ 12.4, 19.1, 21.6, 29.2, 64.7, 65.1, 72.4, 73.7, 74.8, 75.6, 78.1, 80.2, 101.5, 112.1, 128.3, 128.6, 128.9, 129.0, 131.0, 132.8, 136.7, 139.8, 146.6, 151.7, 164.5; MS (EI) *m/z* (I_{rel},%) 602 (0.6), 430 (1.4), 353 (3.1), 172 (3.7), 155 (8.6), 127 (8.4), 91 (100), 65 (9.1); HRMS (EI): Calcd for $C_{29}H_{34}N_2O_{10}S$ $[M]^+$: 602.1934. Found: 602.1935.

4.4. 1-(3-*O*-Benzyl-4,6-*O*-isopropylidene-2-*O*,5-*C*-methano-β-D-glucopyranosyl)thymine 6

To a solution of compound **5** (478 mg, 0.79 mmol) in DMF (8 mL) was added sodium hydride (95 mg, 60% in oil, 2.4 mmol) and the resultant mixture was stirred at 60 °C for 10 min under a N_2 atmosphere. After addition of saturated aq NH_4Cl, the reaction mixture was extracted with AcOEt. The organic layer was washed with H_2O, and brine, dried over Na_2SO_4, and concentered. The crude product was purified by column chromatography (SiO_2, *n*-hexane/AcOEt = 1:2) to give compound **6** (329 mg, 97%) as a white foam. $[\alpha]_D^{22}$ +14.0 (*c* 1.00, $CHCl_3$); IR ν_{max} (KBr): 1682, 2993 cm^{-1}; ^1H NMR (300 MHz, $CDCl_3$) δ 1.44 (3H, s), 1.55 (3H, s), 1.79 (3H, d, *J* = 1 Hz), 3.65 (1H, d, *J* = 15 Hz), 3.81 (1H, ddd, *J* = 2, 5, 5 Hz), 3.86 (1H, dd, *J* = 2, 13 Hz), 3.95 (1H, d, *J* = 15 Hz), 4.06 (1H, dd, *J* = 2, 5 Hz), 4.39–4.50 (4H, m), 6.14 (1H, t, *J* = 2 Hz), 7.10–7.13 (2H, m), 7.23–7.32 (4H, m), 9.14 (1H, br s); ^{13}C NMR (75.5 MHz, $CDCl_3$) δ 12.7, 18.8, 28.9, 62.9, 65.8, 65.9, 68.6, 72.2, 75.1, 78.6, 83.4, 100.1, 109.1, 127.6, 128.2, 128.6, 135.5, 136.9, 150.2, 164.0; MS (EI) *m/z* (I_{rel},%) 430 (16.8), 415 (4.4), 167 (15.2), 133 (6.2), 127 (10.0), 111 (8.5), 97 (11.4), 91 (100), 69 (7.1); HRMS (EI): Calcd for $C_{22}H_{26}N_2O_7$ $[M]^+$: 430.1740. Found: 430.1770.

4.5. 1-(4,6-*O*-Isopropylidene-2-*O*,5-*C*-methano-β-D-glucopyranosyl)thymine 7

To a solution of compound **6** (134 mg, 0.31 mmol) in AcOEt (6.2 mL) was added 20% $Pd(OH)_2/C$ (67 mg). The reaction mixture was stirred under H_2 atmosphere at room temperature for 20 h, filtered and concentrated. The crude product was purified by column chromatography (SiO_2, *n*-hexane/AcOEt = 1:5) to give compound **7** (100 mg, 94%) as a white foam. $[\alpha]_D^{24}$ −60.1 (*c* 1.00, $CHCl_3$); IR ν_{max} (KBr): 1700, 2993, 3186 cm^{-1}; ^1H NMR (400 MHz, $CDCl_3$) δ 1.43 (3H, s), 1.66 (3H, s), 1.83 (3H, s), 3.66 (1H, d, *J* = 11 Hz), 3.83 (1H, d, *J* = 10 Hz), 4.04 (1H, d, *J* = 11 Hz), 4.24 (2H, s), 4.43 (1H, d, *J* = 10 Hz), 4.50 (1H, m), 4.99 (1H, s), 5.97 (1H, d, *J* = 1 Hz), 7.51 (1H, s), 10.33 (1H, s); ^{13}C NMR (75.5 MHz, $CDCl_3$) δ 12.8, 19.1, 29.0, 63.2, 65.8, 66.9, 68.7, 71.7, 74.6, 84.2, 100.2, 109.8, 135.1, 150.7, 164.6; MS (EI) *m/z* (I_{rel},%) 340 (19.3), 325 (13.4), 214 (100), 185 (13.7), 167 (35.9), 157 (19.9), 139 (13.2), 127 (46.2), 111 (22.5), 97 (24.0), 83 (26.8), 69 (37.6), 59 (50.6); HRMS (EI): Calcd for $C_{15}H_{20}N_2O_7$ $[M]^+$: 340.1271. Found: 340.1273.

4.6. 1-(3-Deoxy-3-exomethylene-4,6-*O*-isopropylidene-2-*O*,5-*C*-methano-β-D-glucopyranosyl)thymine 8

To a solution of compound **7** (89 mg, 0.26 mmol) in CH_2Cl_2 (2.6 mL) were added MS4A (180 mg) and pyridinium dichromate (120 mg, 0.32 mmol) and the resultant mixture was stirred at room temperature for 2 h under a N_2 atmosphere. In a separate flask, triphenylphosphonium bromide (476 mg, 1.33 mmol) was stirred at −78 °C under a N_2 atmosphere in dry THF (3.1 mL), and *n*-butyllithium (1.65 M in *n*-hexane, 0.76 mL, 1.25 mmol) was added dropwise to give a yellow slurry. After stirring the phosphonium ylide for 1 h at 0 °C, it was cooled to −78 °C and was added to the PDC reaction mixture at −78 °C. The reaction mixture was warmed slowly to rt and stirred for 3 h. After filtration of the mixture through a Celite pad, the filtrate was concentrated under reduced pressure. The crude product was purified by column chromatography (SiO_2, *n*-hexane/AcOEt = 1:1) to give compound **8** (53 mg, 61%) as a white foam. $[\alpha]_D^{18}$ +20.8 (*c* 1.00, $CHCl_3$); IR ν_{max} (KBr): 1681, 1696, 2880, 2995, 3190 cm^{-1}; ^1H NMR (400 MHz, $CDCl_3$) δ 1.48 (3H, s), 1.62 (3H, s), 1.95 (3H, d, *J* = 1 Hz), 3.66 (1H, d, *J* = 11 Hz), 3.95–3.98 (2H, m), 4.45 (1H, dd, *J* = 2, 10 Hz), 4.56 (1H, d, *J* = 10 Hz), 5.44 (1H, d, *J* = 3 Hz), 5.51 (1H, d, *J* = 3 Hz), 6.21 (1H, d, *J* = 2 Hz), 7.23 (1H, d, *J* = 1 Hz), 8.89 (1H, br s); ^{13}C NMR (75.5 MHz, $CDCl_3$) δ 13.0, 19.0, 28.9, 63.2, 66.3, 69.2, 69.6, 70.9, 84.2, 100.5, 110.4, 119.7, 133.9, 138.1, 150.1, 163.9; MS (EI) *m/z* (I_{rel},%) 336 (3.1), 321 (5.1), 279 (2.8), 182 (75.2), 167 (69.2), 152 (9.6), 124 (97.8), 95 (100), 67 (68.5); HRMS (EI): Calcd for $C_{16}H_{20}N_2O_6$ $[M]^+$: 336.1321. Found: 336.1320.

4.7. 1-(3-Deoxy-3-exomethylene-2-*O*,5-C-methano-β-D-glucopyranosyl)thymine 9

Compound **8** (55 mg, 0.16 mmol) was dissolved in AcOH/H_2O (3:2, 2.4 mL) and stirred at room temperature for 10 h. The solvent was removed under reduced pressure and the residue co-evaporated with toluene. The crude product was purified by column chromatography (SiO_2, $CHCl_3$/MeOH = 15:1) to give compound **9** (45 mg, 93%) as a white foam. $[\alpha]_D^{23}$ +67.9 (*c* 1.00, CH_3OH); IR ν_{max} (KBr): 1695, 3391 cm^{-1}; ^1H NMR (300 MHz, DMSO-d_6) δ 1.75 (3H, d, *J* = 1 Hz), 3.55 (1H, d, *J* = 16 Hz), 3.55 (1H, d, *J* = 16 Hz), 3.61 (1H, d, *J* = 16 Hz), 3.90–3.93 (1H, m), 3.99 (1H, d, *J* = 13 Hz), 4.20 (1H, d, *J* = 3 Hz), 4.33 (1H, m), 4.88 (1H, br s), 5.29 (1H, s), 5.36 (1H, s), 5.75 (1H, br s), 5.98 (1H, d, *J* = 3 Hz), 7.32 (1H, d, *J* = 1 Hz); ^{13}C NMR (75.5 MHz, CD_3CN) δ 12.5, 62.2, 64.6, 67.2, 72.3, 79.4, 83.8, 109.7, 119.7, 135.9, 143.9, 151.0, 164.7; MS (FAB) *m/z* 297 $[M+H]^+$; HRMS (FAB): Calcd for $C_{13}H_{17}N_2O_6$ $[M+H]^+$: 297.1081. Found: 297.1109.

4.8. 1-{3-Deoxy-6-*O*-(4,4′-dimethoxytrityl)-3-exomethylene-2-*O*,5-C-methano-β-D-glucopyranosyl}thymine 10

To a solution of compound **9** (45 mg, 0.15 mmol) in pyridine (1.5 mL) was added 4,4′-dimethoxytrityl chloride (78 mg, 0.23 mmol) and the resultant mixture was stirred at room temperature for 4 h under a N_2 atmosphere. After addition of H_2O, the reaction mixture was extracted with AcOEt, the organic layer was dried over Na_2SO_4, and concentered. The crude product was purified by column chromatography (SiO_2, 0.5% triethylamine in *n*-hexane/AcOEt = 1:1) to give compound **10** (86 mg, 96%) as a white foam. $[\alpha]_D^{24}$ +39.6 (*c* 1.00, $CHCl_3$); IR ν_{max} (KBr): 1509, 1607,

1693, 2836, 2934, 3003, 3185, 3402 cm^{-1}; ^1H NMR (300 MHz, $CDCl_3$) δ 1.93 (3H, s), 2.38 (1H, d, J = 6 Hz), 3.23 (1H, d, J = 14 Hz), 3.40 (1H, d, J = 14 Hz), 3.80 (6H, s), 3.89 (1H, d, J = 13 Hz), 4.09 (1H, d, J = 13 Hz), 4.46 (1H, d, J = 3 Hz), 4.62 (1H, m), 5.37 (1H, d, J = 2 Hz), 5.53 (1H, m), 6.16 (1H, d, J = 3 Hz), 6.84–6.87 (4H, m), 7.22–7.46 (10H, m), 9.07 (1H, br s); ^{13}C NMR (75.5 MHz, $CDCl_3$) δ 12.9, 30.1, 55.3, 62.2, 64.4, 67.2, 71.1, 78.0, 83.4, 86.6, 109.8, 113.4, 119.9, 127.2, 128.0, 128.1, 130.0, 130.1, 134.7, 135.3, 135.4, 141.8, 144.5, 150.2, 158.7 (1), 158.7 (4), 164.2; MS (FAB) m/z 599 $[M+Na]^+$; HRMS (FAB): Calcd for $C_{34}H_{35}N_2O_8$ $[M+H]^+$: 599.2388. Found: 599.2427.

4.9. 1-[4-*O*-{2-Cyanoethoxy(diisopropylamino)phosphino}-3-deoxy-6-*O*-(4,4′-dimethoxytrityl)-3-exomethylene-2-*O*,5-*C*-methano-β-D-glucopyranosyl]thymine 11

To a solution of compound **10** (74 mg, 0.12 mmol) in dry CH_3CN (1.2 mL) were added *N*,*N*-diisopropylethylamine (63 μL, 0.36 mmol) and 2-cyanoethyl *N*,*N*-diisopropylphosphoramidochloridite (40 μL, 0.18 mmol) and the resultant mixture was stirred at 0 °C for 2.5 h under a N_2 atmosphere. Further *N*,*N*-diisopropylethylamine (21 μL, 0.12 mmol) and 2-cyanoethyl *N*,*N*-diisopropylphosphoramidochloridite (13 μL, 0.06 mmol) were added to the mixture and the mixture was stirred at 0 °C for 1.5 h. The reaction mixture was concentrated and the obtained crude product was purified by column chromatography (SiO_2, 0.5% triethylamine in *n*-hexane/AcOEt = 1:1) to give compound **11** (76 mg, 79%) as a white foam. ^{31}P NMR (161.8 MHz, $CDCl_3$) δ 149.3, 149.8; MS (FAB) m/z 799 $[M+H]^+$; HRMS (FAB): Calcd for $C_{43}H_{52}N_4O_9P$ $[M+H]^+$: 799.3466. Found: 799.3491.

4.10. Oligodeoxynucleotide 12

Synthesis of ODN **12** modified with BsNA **2** was performed on an automated DNA synthesizer (Gene Design nS-8) on a 0.2 μmol scale using a phosphoramidite coupling protocol and 5-[3,5-bis(trifluoromethyl)phenyl]-1*H*-tetrazole as the activator. The concentration of each phosphoramidite was 0.1 M and the coupling times were 8 min. Coupling yields were checked by trityl monitoring and were estimated to be over 95%. The CPG solid supported ODN (DMTr-ON) was treated with concentrated ammonium hydroxide solution at 55 °C for 12 h, and then concentrated. The crude ODN was roughly purified and detritylated with a Sep-Pak Plus C_{18} Environmental Cartridge, and then carefully by RP-HPLC using Waters XBridge™ OST C18 2.5 μm (10 × 50 mm) with a linear gradient of CH_3CN (6–12% over 30 min) in 0.1 M triethylammonium acetate buffer (pH = 7.0). The purity of the ODN was analyzed by RP-HPLC on a Waters XBridge™ Shield RP 18 2.5 μm (4.6 × 50 mm) and characterized by MALDI-TOF mass spectrometry. The isolation yield calculated from the UV absorbance at 260 nm was 27%. MALDI-TOF-MS data ($[M-H]^-$): found 3688.5 (calcd 3687.4).

Acknowledgments

This study was supported by the Japan Society for the Promotion of Science (JSPS), the Ministry of Education, Culture, Sports, Science, and Technology in Japan (MEXT), and the Advanced Research for Medical Products Mining Programme of the National Institute of Biomedical Innovation (NIBIO). K.M. is grateful for a Research Fellowship for Young Scientist from JSPS.

Supplementary data

Supplementary data associated with this article can be found, in the online version, at http://dx.doi.org/10.1016/j.bmc.2014.11.030.

References and notes

1. (a) Rahman, S. M. A.; Imanishi, T.; Obika, S. *Chem. Lett.* **2009**, *38*, 512; (b) Obika, S.; Rahman, S. M. A.; Fujisaka, A.; Kawada, Y.; Baba, T.; Imanishi, T. *Heterocycles* **2010**, *81*, 1347; (c) Prakash, T. P. *Chem. Biodivers.* **2011**, *8*, 1616.
2. Obika, S.; Nanbu, D.; Hari, Y.; Morio, K.; In, Y.; Ishida, T.; Imanishi, T. *Tetrahedron Lett.* **1997**, *38*, 8735.
3. Singh, S. K.; Nielsen, P.; Koshkin, A. A.; Wengel, J. *Chem. Commun.* **1998**, 455.
4. (a) Veedu, R. N.; Wengel, J. *Chem. Biodivers.* **2010**, *7*, 536; (b) Yamamoto, T.; Nakatani, M.; Narukawa, K.; Obika, S. *Future Med. Chem.* **2011**, *3*, 339.
5. Østergaard, M. E.; Hrdlicka, P. J. *Chem. Soc. Rev.* **2011**, *40*, 5771.
6. (a) Seth, P. P.; Allerson, C. R.; Berdeja, A.; Siwkowski, A.; Pallan, P. S.; Gaus, H.; Prakash, T. P.; Watt, A. T.; Egli, M.; Swayze, E. E. *J. Am. Chem. Soc.* **2010**, *132*, 14942; (b) Hanessian, S.; Schroeder, B. R.; Giacometti, R. D.; Merner, B. L.; Østergaard, M. E.; Swayze, E. E.; Seth, P. P. *Angew. Chem., Int. Ed.* **2012**, *51*, 11242; (c) Morihiro, K.; Kodama, T.; Kentefu; Moai, Y.; Veedu, R. N.; Obika, S. *Angew. Chem., Int. Ed.* **2013**, *52*, 5074.
7. (a) Hari, Y.; Obika, S.; Ohnishi, R.; Eguchi, K.; Osaki, T.; Ohishi, H.; Imanishi, T. *Bioorg. Med. Chem.* **2006**, *14*, 1029; (b) Mitsuoka, Y.; Kodama, T.; Ohnishi, R.; Hari, Y.; Imanishi, T.; Obika, S. *Nucleic Acids Res.* **2009**, *37*, 1225.
8. (a) Mori, K.; Kodama, T.; Obika, S. *Org. Lett.* **2011**, *13*, 6050; (b) Migawa, M. T.; Seth, P. P.; Swayze, E. E.; Ross, B. S.; Song, Q.; Han, M. PCT Int. Appl. WO 2011/017521 A2, 2011.
9. Bomholt, N.; Jørgensen, P. T.; Pedersen, E. B. *Bioorg. Med. Chem. Lett.* **2011**, *21*, 7376.
10. Madsen, A. S.; Wengel, J. *J. Org. Chem.* **2012**, *77*, 3878.
11. Matsuda, A.; Sasaki, T. *Cancer Sci.* **2004**, *95*, 105.
12. (a) Buchanan, J. G.; Wightman, R. H. In *Topics in Antibiotic Chemistry*; Sammes, P. G., Ed.; Ellis Horwood: West Sussex, 1982; Vol. 6, p 229; (b) Nakagawa, F.; Okazaki, T.; Naito, A.; Iijima, Y.; Yamazaki, M. *J. Antibiot.* **1985**, *38*, 823; (c) Takahashi, S.; Nakagawa, F.; Kawazoe, K.; Furukawa, Y.; Sato, S.; Tamura, C.; Naito, T. *J. Antibiot.* **1985**, *38*, 830.
13. Takenuki, K.; Matsuda, A.; Ueda, T.; Sasaki, T.; Fujii, A.; Yamaguchi, K. *J. Med. Chem.* **1988**, *31*, 1063.
14. Seth, P. P.; Allerson, C. R.; Berdeja, A.; Swayze, E. E. *Bioorg. Med. Chem. Lett.* **2011**, *21*, 588.

Organic LETTERS

Letter

pubs.acs.org/OrgLett

Sulfonamide-Bridged Nucleic Acid: Synthesis, High RNA Selective Hybridization, and High Nuclease Resistance

Yasunori Mitsuoka,[†,‡] Yuko Fujimura,[‡] Reiko Waki,[†] Akira Kugimiya,[‡] Tsuyoshi Yamamoto,[†] Yoshiyuki Hari,[†] and Satoshi Obika*[,†]

[†]Graduate School of Pharmaceutical Sciences, Osaka University, 1-6 Yamadaoka, Suita, Osaka 565-0871, Japan

[‡]Discovery Research Laboratory for Innovative Frontier Medicines, Shionogi & Co., Ltd., 3-1-1 Futaba-cho, Toyonaka, Osaka 561-0825, Japan

Supporting Information

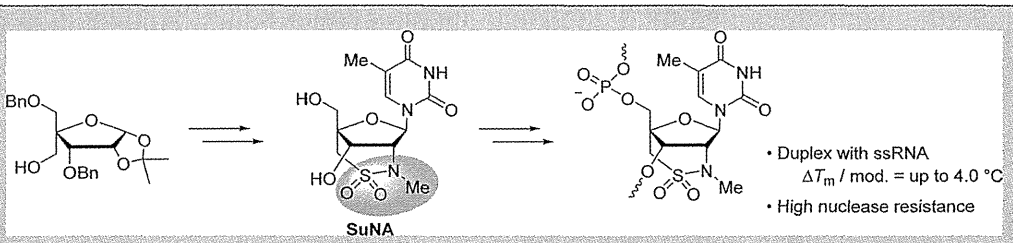

ABSTRACT: 2′-*N*,4′-*C*-(*N*-Methylamino)sulfonylmethylene-bridged thymidine (SuNA), which has a six-membered linkage including a sulfonamide moiety, was synthesized and introduced into oligonucleotides. The oligonucleotides containing SuNA exhibited excellent nuclease resistance, a high affinity toward single-stranded RNA, and a low affinity toward single-stranded DNA compared to the natural oligonucleotide.

The first systemic antisense drug, Kynamro, was approved by the FDA in 2013,[1] and many other antisense oligonucleotides are in clinical trials. For the practical application of antisense methodology, chemical modification is essential to achieve a strong interaction with single-stranded RNA (ssRNA) in a sequence-specific manner. In addition, high resistance against enzymatic degradation is also required for in vivo applications. Among numerous chemical modifications, the introduction of a bridged structure between the 2′- and 4′-positions generally increases affinity toward ssRNA and improves resistance to nuclease degradation.[2] Since the discovery of the 2′-*O*,4′-*C*-methylene-bridged nucleic acid (2′,4′-BNA[3]/LNA[4]), which is a typical example of these bridged compounds, many bridged nucleic acids have been developed.[5−11] Previous studies have revealed that nuclease resistance can be enhanced by increasing the ring size of the bridge moieties because of increasing steric hindrance (i.e., 2′,4′-BNA/LNA < ENA,[5] 2′,4′-BNA^{NC}[6] < 2′,4′-BNA^{COC}[7]) (Figure 1). However, this decreases binding affinity because of insufficient restriction of the sugar conformation (i.e., 2′,4′-BNA/LNA > ENA, 2′,4′-BNA^{NC} > 2′,4′-BNA^{COC}). Thus, a balance between these two properties would be very important for the development of practical antisense oligonucleotides.

Recently, we synthesized several 2′,4′-BNAs possessing amide or urea moieties in their bridged structure (Figure 1). They possessed increased nuclease resistance and/or RNA selectivity compared to analogues with the same-membered bridged structure, maintaining high affinity toward ssRNA (i.e., 2′,4′-BNA/LNA vs AmNA,[8] ENA vs six-membered AmNA,[9] 2′,4′-BNA^{COC} vs urea-BNA[10]). These properties suggest that

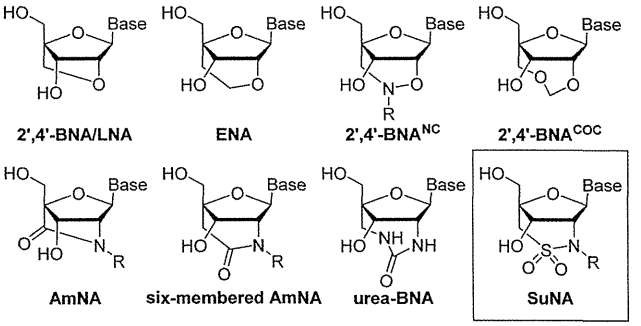

Figure 1. Structures of 2′,4′-BNA/LNA, ENA, 2′,4′-BNA^{NC}, 2′,4′-BNA^{COC}, AmNA, six-membered AmNA, urea–BNA, and SuNA designed in the present study.

the exocyclic carbonyl groups inhibit the interaction between the oligonucleotides and nuclease and destabilize the duplex formed with single-stranded DNA (ssDNA). These are expected to derive from steric and electronic properties of the exocyclic carbonyl groups. However, how the bridged moiety itself affects the hybridization properties and the nuclease resistance of the oligonucleotides remains unknown.

This study used a sulfonamide structure, which is often seen in bioactive compounds or drugs,[12] to evaluate the relationship between ring size and hybridization properties with ssRNA and between bulkiness of the bridge structure and nuclease resistance. Ring size of the bridge structure containing a

Received: September 13, 2014
Published: October 24, 2014

sulfonamide moiety should be larger than that of a same-membered bridged structure because sulfur is larger than oxygen, carbon, or nitrogen. Moreover, a sulfonamide moiety is more bulky than an amide or urea structure. Thus, 2′-*N*,4′-*C*-(*N*-methylamino)sulfonylmethylene-bridged thymidine (SuNA-T) (Figure 1) was synthesized, and the properties of the SuNA-T-modified oligonucleotides were examined.

Initially, the construction of a sulfonamide-bridged structure from **1**,[13] a common precursor for the synthesis of 2′,4′-BNA/LNA, was attempted without any *N*-substituents (Scheme 1). A

Scheme 1. Synthesis of Intermediates and Introduction of Base

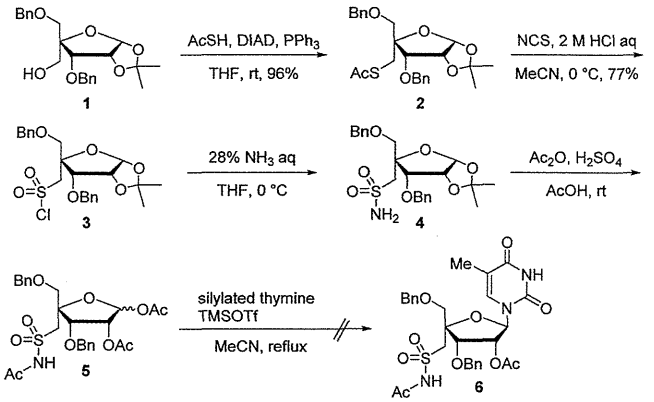

thioacetyl group was introduced into **1** through a Mitsunobu reaction to afford **2**, which was then converted to the sulfonyl chloride derivative **3**.[14] Treatment of **3** with ammonia gave the sulfonamide derivative **4**. In the acetolysis of **4**, the sulfonamide and two hydroxy groups were acetylated to afford triacetate **5**. Although the coupling reaction of **5** with silylated thymine, prepared in situ from thymine and *N*,*O*-bis(trimethylsilyl)-acetamide, was attempted, a complex mixture resulted instead of the desired product **6**. Reactivity of the acylsulfonamide group of **5** may cause many side reactions. This result implied that the construction of a sulfonamide-bridged structure without any *N*-substituents was difficult via this synthetic route.

To avoid the side reactions promoted by the acylsulfonamide group of **5**, a methyl group was introduced into the nitrogen atom of the acylsulfonamide group (Scheme 2). Treatment of **3** with methylamine and subsequent acetolysis afforded triacetate **7**. As expected, the coupling reaction of **7** with silylated thymine was successful and provided the desired product **8** in good yield (74% in three steps), indicating **7** is a good precursor for coupling reactions with silylated nucleobases. After removal of the acetyl groups of **8**, the 2′-hydroxyl group was inverted by mesylation, followed by treatment with NaOH to afford compound **9**. Triflation of **9** and subsequent treatment with K_2CO_3 resulted in intramolecular cyclization to give the desired product **10**. Benzyl groups were removed by hydrogenolysis to afford SuNA-T monomer **11**. Finally, dimethoxytritylation of **11** with 4,4′-dimethoxytrityl chloride followed by phosphitylation gave the phosphoramidite **13**.

The structure of SuNA-T monomer **11**[15] was confirmed by X-ray crystallography (Figure 2a, Table 1). The crystal structure of **11** revealed that the pseudorotation phase angle *P* was 16°, which supports its N-type sugar pucker. Moreover, the ν_{max} and δ values of **11** were 44° and 80°, respectively. The ν_{max} values, which represent the maximum degree of the sugar puckering mode (N/S-type), indicated that the sugar conformation of

Scheme 2. Synthesis of Phosphoramidite 13

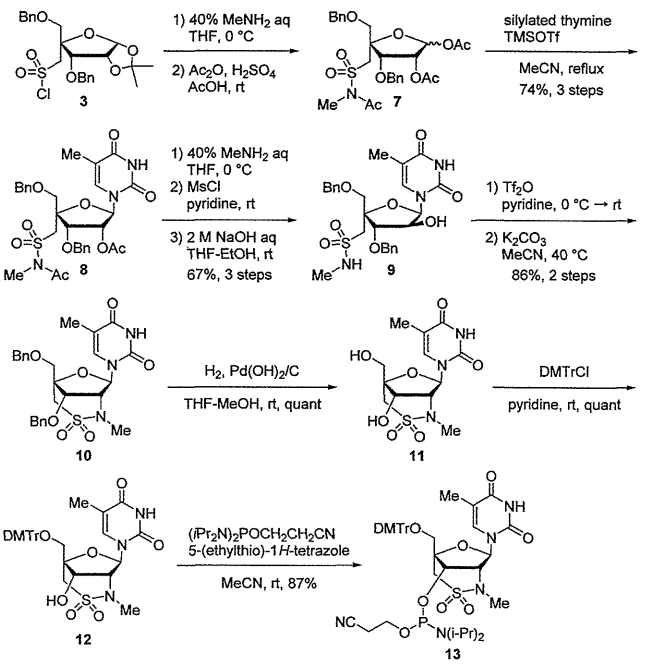

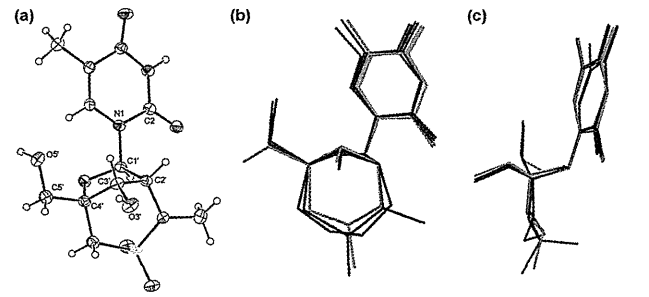

Figure 2. (a) X-ray structure of SuNA-T (**11**). (b, c) Superpositions of X-ray structure of SuNA-T (**11**) (red), 2′,4′-BNA^{NC}[NMe] (green), and 2′,4′-BNA^{COC} (blue).

Table 1. Selected Parameters from X-ray Analysis

		δ (deg)	ν_{max} (deg)	*P* (deg)
2′,4′-BNA		66	57	17
ENA		76	48	15
2′,4′-BNA^{NC}[NMe]		75	49	23
SuNA-T (**11**)	this work	80	44	16
2′,4′-BNA^{COC}		78	38	17

SuNA (ν_{max} 44°) was between the six-membered bridge (ENA and 2′,4′-BNA^{NC}) and the seven-membered bridge (2′,4′-BNA^{COC}) (Figure 2b,c). This may be due to the large sulfur atom. The bridge structure of SuNA is more bulky than that of 2′,4′-BNA^{NC}[NMe], which has the same six-membered bridged structure, because of the two oxygen atoms and methyl group of the sulfonamide moiety (Figure 2b,c).

Phosphoramidite **13** was incorporated into oligonucleotides using an automated DNA synthesizer with standard phosphoramidite chemistry, except for a prolonged coupling time of 16 min with 5-(ethylthio)-1*H*-tetrazole as an activator, conditions similar to those for 2′,4′-BNA^{COC} (see the Supporting Information). The sulfonamide bridge was stable under conventional conditions, that is, aqueous ammonia and

methylamine at room temperature, for cleavage from the resin and removal of protecting groups.

The duplex-forming abilities of the modified oligonucleotides **15**–**19** with ssDNA and ssRNA were evaluated by UV melting experiments and compared with those of the corresponding natural DNA **14** (Table 2). The T_m values for duplexes formed

Table 2. T_m Values (°C) of Oligonucleotides with Complementary DNA and RNA[a]

oligonucleotides	T_m (ΔT_m/mod.) ssDNA	T_m (ΔT_m/mod.) ssRNA	$T_{m\,(RNA)} - T_{m\,(DNA)}$
5′-GCGTTTTTTGCT-3′ (**14**)	53	49	−4
5′-GCGTTTTTTGCT-3′ (**15**)	49 (−4.0)	51 (+2.0)	+2
5′-GCGTTTTTTGCT-3′ (**16**)	47 (−3.0)	54 (+2.5)	+7
5′-GCGTTTTTTGCT-3′ (**17**)	46 (−2.3)	60 (+3.7)	+14
5′-GCGTTTTTTGCT-3′ (**18**)	48 (−1.7)	57 (+2.7)	+9
5′-GCGTTTTTTGCT-3′ (**19**)	53 (0.0)	73 (+4.0)	+20

[a]UV melting profiles were measured in 10 mM sodium phosphate buffer (pH 7.2) containing 100 mM NaCl at a scan rate of 0.5 °C/min at 260 nm. The concentration of the oligonucleotide was 4 μM for each strand. T = SuNA-T. The sequences of target DNA and RNA complements were 5′-d(AGCAAAAAACGC)-3′ and 5′-r-(AGCAAAAAACGC)-3′.

by **15**–**19** with ssRNA were higher than that of the duplex formed by the natural DNA **14** and ssRNA. Changes in ΔT_m/modification values ranged from +2.0 °C to +4.0 °C. This stabilization is between the six-membered bridge (ENA; +3.5 °C to +5.2 °C, 2′,4′-BNA^{NC}; +4.7 °C to +5.8 °C, the six-membered AmNA; +1.0 °C to +4.7 °C) and the seven-membered bridge (2′,4′-BNA^{COC}; +1.0 °C to +2.0 °C and urea-BNA; +1.0 °C to +2.3 °C). This tendency seems to correlate the ν_{max} values of the sugar conformations. In contrast, the oligonucleotides **15**–**19** destabilized the duplex with ssDNA. In the case of **17** and **19**, the differences in T_m values with ssRNA and with ssDNA were 14 and 20 °C, respectively. The oligonucleotides modified by SuNA-T monomer **11** exhibited greater RNA selective hybridization ability than the six-membered AmNA and urea–BNA. This result indicates that a bulky bridge structure destabilized the duplex with ssDNA more efficiently than a small bridge structure, because the bulky bridge would make a steric clash with the C5′ atom of the 3′-neiboring residue when it is located in the narrow minor groove of the B-form DNA duplex.

The enzymatic stability of the modified oligonucleotides was evaluated using a 3′-exonuclease. A comparison of oligonucleotides **20**–**24** is shown in Figure 3. Under the conditions used in this experiment, natural oligonucleotide **20** and the 2′,4′-BNA(LNA)-modified oligonucleotide **21** were completely degraded within 2 and 10 min, respectively. In contrast, the SuNA-modified oligonucleotide **24** significantly enhanced stability against the 3′-exonuclease. This ability was comparable to that of the 2′,4′-BNA^{COC}-modified oligonucleotide **23**, which had a seven-membered bridge structure and was better than that of the 2′,4′-BNA^{NC}[NMe]-modified oligonucleotide **22**, which had a six-membered bridge structure. These results revealed that the six-membered bridged structure possessing a

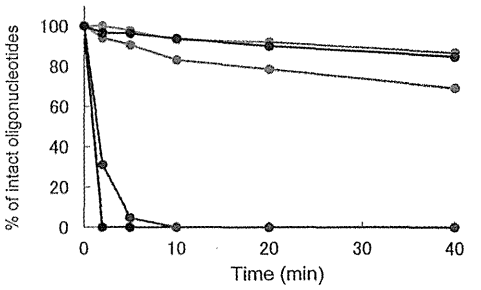

Figure 3. Hydrolysis of oligonucleotides (750 pmol) conducted at 37 °C in buffer (100 μL) containing 50 mM Tris-HCl (pH 8.0), 10 mM $MgCl_2$, and phosphodiesterase I (4.0 μg/mL). Sequences: 5′-d(TTTTTTTTTT-3′, T = natural (black, **20**), 2′,4′-BNA/LNA (pink, **21**), 2′,4′-BNA^{NC}[NMe] (green, **22**), 2′,4′-BNA^{COC} (blue, **23**), SuNA (red, **24**).

sulfonamide moiety inhibited degradation by a 3′-exonuclease as well as the seven-membered bridge structure did. Previous modeling studies suggested that the appropriate bridged structure between the 2′- and 4′-positions causes a steric challenge to nuclease binding, and a steric clash with the metal ion in the active site of the nuclease and consequently this provides high nuclease resistance.[16] We suppose that the sulfonamide bridge can emphasize the steric clash with the nuclease surface and the metal ion and lead to high enzymatic stability.

For the practical application of antisense methodology, the degradation of the complementary RNA through the RNase H mechanism is very important.[17,18] Hence, the SuNA-modified gapmer **25**, which is 16-mer length having 7-mer central DNA gap and fully modified with the phosphorothioate linkages, was synthesized (Table S1, Supporting Information), and the degradation of complementary RNA in the **25**/RNA hetereoduplex was examined in the presence of RNase H (Figure 4).[11g] Under the conditions used in this experiment,

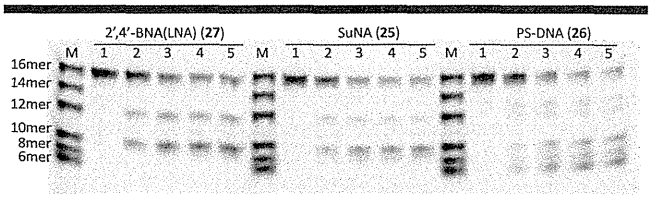

Figure 4. *E. coli* RNase H activity analysis of 5′-Cy3-labeled RNA forming duplexes with phosphorothioated DNA (PS-DNA) **26**, the 2′,4′-BNA(LNA)-modified gapmer **27**, and the SuNA-modified gapmer **25** using 25% denaturing PAGE containing 7 M urea. Lanes 1–5 represent digestion time at 0, 5, 15, 30, and 60 min, respectively. Conditions of cleavage reaction: 5′-Cy3-labeled RNA (0.5 μM) and **25**-**27** (10 μM) in reaction buffer containing 40 mM Tris-HCl (pH 7.2), 150 mM NaCl, 4 mM $MgCl_2$, and 1 mM DTT at 37 °C; 0.01 U/μL of RNase H. M: Marker.

degradation of RNA in the **25**/RNA hetereoduplex was observed. A similar degradation was shown in the phosphorothioated DNA (PS-DNA) **26**/RNA and the 2′,4′-BNA(LNA)-modified gapmer **27**/RNA hetereoduplex.

In conclusion, a novel bridged nucleic acid monomer **11**, 2′-*N*,4′-*C*-(*N*-methylamino)sulfonylmethylene-bridged thymidine (SuNA-T), has been designed and successfully synthesized. This is the first example of a nucleic acid analogue with a sulfonamide-type bridged structure between the 2′- and 4′-positions. The SuNA-modified oligonucleotides produced